



Temporal evolution of cosmological density perturbations of the Bose–Einstein condensate dark matter

Subhra Mondal^a, Amitava Choudhuri^b

Department of Physics, The University of Burdwan, Golapbag, Purba Bardhaman, West Bengal 713104, India

Received: 31 October 2023 / Accepted: 11 February 2024

© The Author(s) 2024

Abstract Dark matter is assumed to be composed of scalar boson particles that form Bose–Einstein condensate during the cosmic evolution of the Universe when the temperature of the dark matter is below the critical temperature T_{cr} . At around a redshift $z \sim 1200$, the normal dark matter converted to Bose–Einstein condensate dark matter through a first-order phase transition and continued to complete the condensation process for nearly 10^6 years, until then, both phases coexist. In this manuscript, considering Bose–Einstein condensate dark matter as a Gross–Pitaevskii–Poisson system, we study the time evolution of density contrast of Bose–Einstein condensate dark matter using cosmological linear perturbation theory following previous works on the subject. The evolution equation contains quantum pressure due to Heisenberg’s uncertainty principle and self-interaction pressure terms. We solve the temporal density contrast equation of Bose–Einstein condensate dark matter analytically for both the Thomas–Fermi limit and the non-interacting case where the expansion rule follows similarly to that of the Einstein–de Sitter Universe. In addition, we also numerically analyze the temporal nature of the evolution of density contrast of Bose–Einstein condensate dark matter for the complete equation without applying any approximation. We find that the Bose–Einstein condensate model of dark matter could modify the temporal nature of density contrast evolution due to the presence of self-interaction and quantum pressure terms, which shows significant differences with respect to the conventional standard cold dark matter, and successfully solves the small-scale problems in the context of cosmological structure formation.

1 Introduction

The large-scale structure formation of the Universe is a major problem of cosmology. The journey of translation from a homogeneous and isotropic early Universe to the vastly clumped present Universe is fascinating. In the inflationary phase of the early Universe, a small quantum fluctuation in scalar curvature laid the seed of cosmological structure formation. Afterward, the small fluctuation is stretched by the rapid expansion of the Universe during inflation and subsequently amplified through gravitational (Jeans) instability and gives rise to structures we observe today [1,2]. Though Sir Jeans [3,4] in 1902 introduced the first sincere theory of galaxy formation for the non-relativistic fluid, it did not incorporate the effect of the expansion of the Universe. Later Lifshitz [5] in 1946 had given a satisfactory relativistic theory of the formation of structures in an expanding Universe. He had shown the power law of growth instead of exponential as suggested in Jeans’s theory. Later in 1957, Bonnor [6] suggested a non-relativistic approach to the same. Cosmological observations of distant type Ia supernovae provide data suggesting that the Universe is made of about 70% dark energy (DE), 25% dark matter (DM), and 5% visible matter (baryons) [7,8]. The dark sector, which consists of almost 95% of the total, can hardly be detected through direct observations. The DE (cosmological constant Λ), which is thought of as a form of zero-point or vacuum energy, has negative pressure and is responsible for the present acceleration of the Universe. An extensive category of particle physics candidates of DM is non-baryonic, non-relativistic, and weakly-interacting massive particles (WIMPs). There are several other speculative candidates of DM such as standard model neutrinos, sterile neutrinos, axions, and supersymmetric candidates (e.g. neutralinos, gravitinos, axinos, etc), etc, albeit the actual nature of DM is still mysterious [9–11]. The only shreds of evi-

^a e-mail: cosmology313@gmail.com

^b e-mail: amitava_ch26@yahoo.com (corresponding author)

dence of DM are from galactic rotation curves [12, 13] and gravitational lensing [14].

The cosmological concordance Λ CDM model, known as the standard model of contemporary cosmology is made of DE, cold dark matter (CDM), and ordinary baryonic matter components. It has proven remarkably successful in elucidating various aspects of cosmology, ranging from the late-time acceleration of the expanding Universe [7, 15] to the statistical characteristics and power spectrum of cosmic microwave background (CMB) anisotropy [16]. The model also effectively describes the characteristics of extensive cosmic structures in the Universe [17, 18] as well as the observed prevalence of light nuclei such as hydrogen, helium, and others [19–22]. Although the Λ CDM model has achieved impressive triumphs and offers a straightforward framework, presently its validity is subject to rigorous scrutiny as discussed in Refs. [23–27]. This arises from various significant theoretical and observational challenges confronting the model. Such shortcomings are the so-called cosmological constant problem which is related to the apparent mismatch between the observed value of the cosmological constant and the theoretical expectations based on our understanding of quantum field theory [28–30], and the late time coincidence problem referring to the puzzling observation that the energy densities of DM and DE in the Universe are of the same order of magnitude almost recently at a redshift $z \approx 0.55$, even though they have evolved differently over cosmic time [31, 32]. Furthermore, there are other important anomalies such as the Hubble tension [27, 33, 34], cosmic microwave background (CMB) anisotropy anomalies [35, 36], baryon acoustic oscillations (BAO) curiosities [37–39], etc. (see Ref. [40] for details). At scales smaller than a few hundred kpc, certain aspects of the predictions made by the Λ CDM model appear to deviate from what is observed in several instances [41–43]. Especially when examining galaxies, observations highlight several challenges that the Λ CDM model encounters when trying to explain structures on smaller scales, specifically those below approximately 1 Mpc [44–46]. The ‘core-cusp problem’ [47–50] highlights a notable disparity. This discrepancy emerges within the density profile of the DM halo in low-mass galaxies, as depicted by N -body simulations which is a crucial method in physical cosmology for assessing the predictions of the Λ CDM model. This profile is conventionally characterized as having cusp-like behavior [51–54]. Contrasting this, there is the observed astronomical density profile of low surface brightness galaxies, which typically showcases a core configuration [55–58]. The ‘missing satellites problem’, also known as the dwarf galaxy problem [59–62], underscores a notable excess. It stems from a notable deviation between the projected count of substructures within halos as predicted by comprehensive collisionless N -body simulations and the actual count of satellite galaxies observed within the Local Group. Notably,

the Λ CDM model forecasts a significantly greater number of satellites often on the order of thousands compared to the comparatively smaller count of observed dwarf galaxies, which typically hovers around fifty [61, 63].

The last two aforementioned small-scale problems are important to us in the context of structure formation. The challenges posed by the core-cusp and overabundance of satellite galaxies issues can be figured out by considering alternative scenarios. In 2000 Spergel and Steinhardt [64] proposed a solution to the problems of the Λ CDM model by considering DM as a non-dissipative, cold, but self-interacting except small scattering cross-section. Hu et al. [65] in 2000 suggested that DM is made up of extremely lightweight free scalar particles. These particles would have masses around 10^{-22} eV and would start off forming a cold Bose–Einstein condensate (BEC). This concept is often referred to as ‘fuzzy cold dark matter’ (FCDM). The inherent wave properties of ultralight DM have the capacity to obstruct the development of kpc-scale cusps within DM halos, simultaneously diminishing the prevalence of halos with lower masses. In 2015 Suárez and Chavanis [66] considered the self-interacting complex scalar field dark matter (SFDM) model, represented by the Klein–Gordon–Einstein (KGE) equations. Within the framework of the SFDM model, there exists an inherent small-scale finite Jeans cut-off length linked to the principles of quantum mechanics, which could potentially solve the missing satellite problem. On the other hand, the emergence of the quantum potential, originating from the Heisenberg uncertainty principle in the case of a noninteracting scalar field (SF), or from the pressure resulting from scattering in the case of a self-interacting SF, serves as a barrier against gravitational collapse on small scales. Consequently, this phenomenon gives rise to central density cores as opposed to cusps.

In the context of the possibility of having bosonic structures, there exists a lot of studies. In 1990 Press et al. [67] studied small-scale and large-scale structures with soft-boson particles in which baryons are gravitationally coupled considering a bosonic complex SF with quadratic and quartic self-coupling. They showed that Heisenberg’s uncertainty principle prevents soft-bosonic matter from falling into galaxy clusters and thus solves the problem of dark missing matter. Frieman et al. [68] in 1992, based on particle physics, describe an important physical phenomenon, the so-called ‘Late time cosmological phase transition’ involving ultralow-mass bosons (pseudo-Nambu–Goldstone bosons). They identified the regions of parameter space by analyzing the cosmic evolution of the aforesaid bosonic field and concluded that it can make a significant contribution to the energy density of the Universe. In 1994 Sin [69] studied the formation of galactic halo quantum mechanically with pseudo-Nambu–Goldstone bosonic DM appeared in late-time cosmological phase transition and followed by an investigation

of galaxy rotation curves in another work [70] by employing Landau–Ginzberg type theory.

It is assumed that the DM is composed of scalar boson particles. Therefore, there is a possibility that the DM could be in the form of BEC at some time in cosmic history, where the mass and scattering length of particles are free parameters to describe the system. In this regard, it is noteworthy that, at very small temperatures, all particles of dilute quantum Bose gas abruptly grow their population in the same ground state and form condensate. For an ideal gas, the BEC process was first predicted in 1924 [71, 72]. Experimental realization of BEC for trapped dilute Bose gases (such as atomic vapor of rubidium and lithium) are reported in Refs. [73–75]. The idea that DM could form BEC was first proposed in Ref. [76] and later reinvestigated in different contexts in different articles [65, 77–80]. Böhmer and Harko [81] in 2007 first went through an in-depth study on the gravitationally trapped condensate DM halos, modeled by Gross–Pitaevskii–Poisson (GPP) system. In the cosmological context, the idea of BEC structure formation is not new (see Refs. [82–91] for details). Crăciun and Harko showed that the data of Spitzer Photometry and Accurate Rotation Curves (SPARC), which includes the database of 173 galaxies gives a good agreement with the theoretical prediction for the slowly rotating BEC model [13]. The nature of DM is hypothetical, i.e. till now we do not know about its behavior properly. It is considered, at the early stage the Universe comprises visible baryonic matter, radiation, DE, and normal DM. The normal DM started converting to the BEC phase through a first-order phase transition as the Universe cooled down below the critical temperature T_{cr} at a redshift $z \sim 1200$ and it takes around 10^6 years to transform into BEC [84]. The purpose of our article is to study the cosmological dynamics of DM in the Universe, specifically, investigating the evolution of density contrast of the BEC DM in an expanding homogeneous and isotropic background from the post-BEC phase to today. To the best of our knowledge, we summarize the research works which are already been accomplished in the context of the evolution of density perturbation of BEC DM as follows. In 2009, Sikivie and Yang [92] showed that self-interacting axions could form BEC after thermalization. They made a relative comparison between the CDM and the axion BEC relating to the behavior of their density perturbations. In 2011, Harko [91] studied the cosmological evolution of density contrast with scale factor for non-relativistic DM by using the post-Newtonian hydrodynamical approach, where background pressure of BEC DM and modes of perturbation are considered to be small. Chavanis [82] in 2012 studied a scale factor dependent growth of perturbation of self-gravitating BEC DM in an expanding Universe with and without special relativistic effects. They provided analytical solutions of density contrast as a function of scale factor for the Thomas–Fermi (TF) limit as well as the non-interacting cases when there are no

Special Relativistic effects and numerical solutions for large wavelengths taking care of special relativistic effects. In the same year, Kian and Ling [93] studied the growth of inhomogeneities of BEC scalar-field DM in both Newtonian relativity (NR) and general relativity (GR) by taking a small and constant present-day pressure limit. In particular, they presented the temporal nature of density contrast for very small modes only for the TF approximation due to facing problems in tackling the quantum pressure term. They pointed out the differences in the results between the BEC model and the Standard Cosmology. In 2013 Freitas and Gonçalves [89] studied the linear evolution of density perturbation during the normal DM to BEC DM phase transition process using a gauge-invariant General Relativistic formalism. Suárez and Chavanis [66] worked on the hydrodynamic representation of KGE equations in the weak gravitational field in 2015. In the non-relativistic limit, GPP equations which are usually used to model BEC DM can be recovered. They also discussed growing and oscillatory modes of density contrast as a function of scale factor for the non-relativistic SF or BEC in detail for the TF limit as well as the non-interacting cases by presenting analytical solutions. Numerical solutions as a function of the scale factor for the complete equation with positive and negative scattering are also been analyzed. Nevertheless, a lot of studies on the evolution of density perturbation of BEC DM have been done, we have scopes to explore further in this field.

Here in this work we review and investigate the cosmological evolution of linear density perturbation in the context of BEC DM structure formation, but especially we focus on the temporal evolution of density contrast with respect to cosmic time rather than evolution in terms of scale factor (see Refs. [66, 82, 91] etc.) as we find no appreciable work has been done on temporal behavior related to this topic. Our digression from the previous studies is twofold. First, we exhibit the analytical solutions of the density contrast equation of BEC DM for the non-interacting (non-zero quantum pressure) and the TF limit (both repulsive and attractive scattering with small but variable BEC pressure) cases in terms of cosmic time and interpret the temporal behavior of density contrast of BEC DM in comparison to the standard pressureless CDM for different modes. Secondly, following Ref. [84] we calculate critical redshift, critical time and condensation time, etc. of the phase transition process from normal to BEC DM, and analyze the temporal behavior of BEC DM after the post-condensation phase using BEC parameters and give a precise understanding of the temporal evolution of the density contrast in the context of the formation of BEC structures in terms of growing and oscillatory solutions. In addition, we also provide the numerical solutions of the density contrast equations and investigate the nature of temporal evolution of the density contrast of the self-interacting BEC DM beyond the TF limit for both repulsive and attractive scattering cases.

We organize the manuscript as follows. In Sect. 2 we model BEC DM as a GPP system and extract quantum hydrodynamic equations following Refs. [81, 94, 95]. Newtonian cosmology for the Einstein-de Sitter (E-dS) Universe is discussed in Sect. 3. Density perturbations in the homogeneous and isotropic background in the expanding Universe scenario are reviewed in Sect. 4 and the obtained perturbed equations are linearized in Sect. 5. The last three sections are summarized from Ref. [82]. In order to measure the evolution of density contrast in terms of cosmic time instead of scale factor, Sect. 6 is devoted to the analytical solutions to the time-evolved linearized evolution equation for the non-interacting and the TF limit cases by following Ref. [82]. Next in Sect. 7, we outline the phase transition process from normal DM to condensate DM from Ref. [84]. In contrast to Ref. [66], analytical results for the two cases as mentioned earlier, and numerical results for self-interacting BEC beyond the TF limit with graphical plots are discussed in Sect. 8 in terms of cosmic time. Finally, we conclude our work in Sect. 9.

2 BEC DM as a GPP system

BEC is based on the wave properties of particles. All the particles are associated with de-Broglie wavelengths $\lambda_{dB} = \sqrt{2\pi\hbar^2/mk_B T}$, where \hbar and k_B are the Planck's constant and Boltzmann's constant respectively, m is the mass and T is the temperature of the condensate particles. If particles of density ρ are cooled down to a certain temperature, called critical temperature $T_{crit} \approx 2\pi\hbar^2\rho^{2/3}/k_B m^{5/3}$, their de-Broglie wavelengths start increasing and eventually exceed the inter-particle separation [84, 89]. At this sufficiently low temperature, the wavelengths overlap with each other and the ground state of the system becomes macroscopically populated. As the system's temperature approaches absolute zero ($T = 0$) a coherent state develops and forms a pure BEC.

It is assumed BEC DM is composed of a weakly interacting ultra-cold dilute gas, in which only low-energy two-body collisions, characterized by *s*-wave scattering length (l_s) is relevant [96]. The dynamics of this system can be well described by the time-dependent Gross-Pitaevskii (GP) equation at $T = 0$, where interaction between particles is treated in the mean-field approximation. The dynamics of gravitationally trapped BEC DM consisting of N numbers of bosonic particles of mass m_χ with non-linear short-range interaction is described by the GPP system [82, 84, 89, 94, 95, 97, 98]

$$\begin{aligned} & -\frac{\hbar^2}{2m_\chi} \vec{\nabla}_r^2 \psi(\vec{r}, t) + m_\chi (V_{grav}(\vec{r}, t) + \zeta(\rho_\chi(\vec{r}, t))) \psi(\vec{r}, t) \\ & = i\hbar \frac{\partial \psi(\vec{r}, t)}{\partial t} \Big|_r, \end{aligned} \quad (1)$$

$$\vec{\nabla}_r^2 V_{grav}(\vec{r}, t) = 4\pi G \rho_\chi(\vec{r}, t), \quad (2)$$

where $\rho_\chi(\vec{r}, t) = N m_\chi |\psi(\vec{r}, t)|^2$ is the density of BEC DM, $V_{grav}(\vec{r}, t)$ is the gravitational trapping potential and G is the universal gravitational constant in the Poisson Eq. (2). $\psi(\vec{r}, t)$ in Eq. (1) denotes the macroscopic wavefunction of the condensate. The non-linear effective potential term in GP Eq. (1) reads [97]

$$\zeta(\rho_\chi(\vec{r}, t)) = \lambda_2 \rho_\chi(\vec{r}, t) + \lambda_3 \rho_\chi^2(\vec{r}, t), \quad (3)$$

where the linear term manifests for two-body interparticle interaction with coupling constant $\lambda_2 = 4\pi\hbar^2 l_s/m_\chi^3$ [82, 98]. In this context, it is to be noted that, encounters among particles at low energies are characterized by the *s*-wave scattering length l_s . The scattering length of dilute BEC clouds is small compared to the inter-particle separation. Therefore only the two-body interactions are dominant. The value of l_s can be both positive and negative based on repulsive and attractive boson-boson interparticle interaction respectively [96]. On the other hand, the quadratic term in (3) accounts for three-body interparticle interaction with coupling constant λ_3 which is important in higher densities, is neglected ($\lambda_3 \approx 0$) in the standard approach of BEC [99, 100]. Making use of the Madelung transformation, we represent the wave function $\psi(\vec{r}, t)$ as [82, 101]

$$\psi(\vec{r}, t) = \sqrt{\rho_\chi(\vec{r}, t)/Nm_\chi} \exp\{i\mathcal{S}(\vec{r}, t)/\hbar\}, \quad (4)$$

where the function $\mathcal{S}(\vec{r}, t)$ in the phase has the dimension of an action. Substituting the transformation (4) into Eq. (1) and separating the imaginary and real parts, we obtain [82]

$$\frac{\partial \rho_\chi(\vec{r}, t)}{\partial t} \Big|_r + \vec{\nabla}_r \cdot \{\rho_\chi(\vec{r}, t) \vec{u}(\vec{r}, t)\} = 0, \quad (5)$$

$$\begin{aligned} \frac{\partial \vec{u}(\vec{r}, t)}{\partial t} \Big|_r + \{\vec{u}(\vec{r}, t) \cdot \vec{\nabla}_r\} \vec{u}(\vec{r}, t) &= -\frac{\vec{\nabla}_r P_\chi(\vec{r}, t)}{\rho_\chi(\vec{r}, t)} \\ & - \vec{\nabla}_r V_{grav}(\vec{r}, t) - \frac{\vec{\nabla}_r V_Q(\vec{r}, t)}{m_\chi} \end{aligned} \quad (6)$$

respectively, with identifying the gradient of pressure, the velocity field of quantum fluid

$$\vec{\nabla}_r P_\chi(\vec{r}, t) = \rho_\chi(\vec{r}, t) \vec{\nabla}_r \zeta, \quad (7a)$$

$$\vec{u}(\vec{r}, t) = \frac{\vec{\nabla}_r \mathcal{S}(\vec{r}, t)}{m_\chi} \quad (7b)$$

respectively, and the quantum potential (due to Heisenberg's uncertainty principle)

$$V_Q(\vec{r}, t) = -\frac{\hbar^2}{2m_\chi} \frac{\vec{\nabla}_r^2 \sqrt{\rho_\chi(\vec{r}, t)}}{\sqrt{\rho_\chi(\vec{r}, t)}}. \quad (8)$$

In deriving Eq. (6), $\mathcal{S}(\vec{r}, t)$ is considered to be non-singular for the sake of simplicity. Due to this, from the identification (7b), we find the condition for irrotational flow $\vec{\nabla}_r \times \vec{u} = 0$

holds good [96]. The Eqs. (5) and (6) are referred as *continuity equation* and *quantum Euler equation* respectively. Hence, it indicates that BEC DM can be described as a non-relativistic Newtonian fluid with quantum effects. In the standard approach of BEC, the equation of state is given by [81, 82, 97]

$$P_\chi(\vec{r}, t) = \zeta \rho_\chi - \int \zeta \, d\rho_\chi = \frac{2\pi l_s \hbar^2}{m_\chi^3} \rho_\chi^2(\vec{r}, t). \quad (9)$$

3 Newtonian cosmology in expanding background

Now we recall the essentials of Newtonian cosmology where the pressure is considered to be negligible in comparison with energy density. We suppose the background¹ is spatially homogeneous of the form

$$\rho_\chi(\vec{r}, t) = \rho_{b\chi}(t), \quad (10a)$$

$$P_\chi(\vec{r}, t) = P_{b\chi}(t), \quad (10b)$$

$$V_{grav}(\vec{r}, t) = V_{b,grav}(\vec{r}, t), \quad (10c)$$

$$\vec{u}(\vec{r}, t) = \vec{u}_b(\vec{r}, t) = H\vec{r}. \quad (10d)$$

Here $H = \dot{S}/S$ is referred to as the time-dependent Hubble parameter, expressing the rate at which the Universe is expanding, and $S(t)$ is the scale factor of the Universe. Subbing Eqs. (10a–10d) in Eqs. (5), (6) and (2), we obtain equations for unperturbed background

$$\frac{d\rho_{b\chi}(t)}{dt} \Big|_r + 3\frac{\dot{S}}{S}\rho_{b\chi}(t) = 0, \quad (11)$$

$$\vec{\nabla}_r V_{b,grav}(\vec{r}, t) = -\frac{\ddot{S}}{S}\vec{r}, \quad (12)$$

and

$$\vec{\nabla}_r^2 V_{b,grav}(\vec{r}, t) = 4\pi G\rho_{b\chi}(t) \quad (13)$$

respectively. The solutions to Eqs. (11) and (12) are

$$\rho_{b\chi} = \frac{\rho_{b0\chi} S_0^3}{S^3}, \quad (14)$$

and

$$V_{b,grav}(\vec{r}, t) = -\frac{1}{2}\frac{\ddot{S}}{S}r^2 \quad (15)$$

respectively, where $\rho_{b0\chi}$ in (14) is the density of the condensate DM for $S = S_0$ (present-day scale factor). Taking divergence of Eq. (12) and using Eq. (13) we obtain

$$\frac{\ddot{S}}{S} = -\frac{4}{3}\pi G\rho_{b\chi}(t). \quad (16)$$

¹ The index b in the suffix denotes unperturbed background quantities.

Now multiplying $2\dot{S}$ to both sides of Eq. (16), using Eq. (14) and integrating we get

$$\left(\frac{\dot{S}}{S}\right)^2 = H^2 = \frac{8\pi G}{3}\rho_{b\chi}(t) - \frac{\kappa}{S^2}, \quad (17)$$

where κ is an integration constant. The Eq. (17) derived in the Newtonian cosmology in an isotropic and homogeneous Universe is the same as the Friedmann equation in GR, provided the pressure is much less than energy density ($P_\chi \ll \rho_\chi c^2$). Also, we can identify κ as the spatial curvature constant used in GR. In such a case, $\kappa = 0$ is for flat space, and $\kappa = \pm 1$ are for elliptical and hyperbolic spaces respectively. From now we shall focus only on the E-dS type Universe which corresponds to² $\kappa = 0$,³ $\Lambda = 0$ and⁴ $P_\chi \ll \rho_\chi c^2$. In that case Eqs. (14) and (17) give

$$S(t) = S_0 \left(\frac{3H_0 t}{2}\right)^{\frac{2}{3}}, \quad (18)$$

$$Ht = \frac{2}{3}, \quad \text{and} \quad \rho_{b\chi}(t) = \frac{1}{6\pi G t^2}.$$

Here H_0 is the Hubble parameter at $S = S_0$.

4 Density perturbations in the expanding Universe

To find the perturbed equations, now we add small perturbations in density ($\delta\rho_\chi(\vec{r}, t)$), pressure ($\delta P_\chi(\vec{r}, t)$), gravitational potential ($\phi(\vec{r}, t)$), and velocity ($\vec{v}(\vec{r}, t)$) to the unperturbed homogeneous background quantities and write

$$\rho_\chi(\vec{r}, t) = \rho_{b\chi}(t) + \delta\rho_\chi(\vec{r}, t), \quad (19a)$$

$$P_\chi(\vec{r}, t) = P_{b\chi}(t) + \delta P_\chi(\vec{r}, t), \quad (19b)$$

$$V_{grav}(\vec{r}, t) = V_{b,grav}(\vec{r}, t) + \phi(\vec{r}, t), \quad (19c)$$

$$\vec{u}(\vec{r}, t) = \vec{u}_b(\vec{r}, t) + \vec{v}(\vec{r}, t). \quad (19d)$$

Substituting (19a–19d) in Eqs. (5), (6) and (2), we obtain a set of equations in perturbed quantities

$$\frac{\partial \delta\rho_\chi}{\partial t} \Big|_r + \rho_{b\chi}(\vec{\nabla}_r \cdot \vec{v}) + \vec{\nabla}_r \cdot (\vec{u}_b \delta\rho_\chi) + \vec{\nabla}_r \cdot (\vec{v} \delta\rho_\chi) = 0, \quad (20)$$

$$\begin{aligned} \frac{\partial \vec{v}}{\partial t} \Big|_r &+ (\vec{u}_b \cdot \vec{\nabla}_r) \vec{v} + (\vec{v} \cdot \vec{\nabla}_r) \vec{u}_b + (\vec{v} \cdot \vec{\nabla}_r) \vec{v} \\ &= -\frac{\vec{\nabla}_r \delta P_\chi}{\rho_{b\chi} + \delta\rho_\chi} - \vec{\nabla}_r \phi + \frac{\hbar^2}{2m_\chi^2} \vec{\nabla}_r \frac{\vec{\nabla}_r^2 \sqrt{1 + \delta\rho_\chi/\rho_{b\chi}}}{\sqrt{1 + \delta\rho_\chi/\rho_{b\chi}}}, \end{aligned} \quad (21)$$

² The inflation theory, introduced by Alan Guth [102] in 1981 as well as the observations [103] both support a flat Universe.

³ From the beginning we have not included cosmological constant term Λ .

⁴ It is under the assumption of Newtonian cosmology.

$$\vec{\nabla}_r^2 \phi = 4\pi G \delta \rho_\chi \quad (22)$$

respectively. In deriving the above equations we have also used the unperturbed set of Eqs. (11–13). So far we have analyzed the system in Eulerian coordinates \vec{r} . As we know the background Hubble flow \vec{u}_b has an explicit dependence on coordinates \vec{r} , the Fourier transformation with respect to the Eulerian coordinates cannot reduce Eqs. (20–22) to a decoupled system of ordinary differential equations. To solve this problem, in the following we use Lagrangian coordinates \vec{x} where the expansion of the Universe is divided out, though the position of matter particles change with time only due to irregular growth of non-uniform distribution of particles caused by gravitational instability. Also, these displacements in position coordinates are the direct consequence of inhomogeneity originated by gravity. Therefore it is essential to recast the perturbed set of equations in the Lagrangian coordinate system. The two coordinate systems and also their gradients and partial time derivatives are related by [104–106]

$$\vec{r} = S\vec{x}, \quad (23a)$$

$$\vec{\nabla}_r = \frac{1}{S} \vec{\nabla}_x, \quad (23b)$$

$$\frac{\partial}{\partial t} \Big|_r = \frac{\partial}{\partial t} \Big|_x - H(\vec{x} \cdot \vec{\nabla}_x) \quad (23c)$$

respectively. Switching (23a–23c) into Eqs. (20–22), and after simplification, we arrive

$$\frac{\partial \delta}{\partial t} \Big|_x + \frac{1}{S} \vec{\nabla}_x \cdot ((1 + \delta) \vec{v}) = 0, \quad (24)$$

$$\left(\frac{\partial}{\partial t} \Big|_x + \frac{\vec{v} \cdot \vec{\nabla}_x}{S} + H \right) \vec{v} = -\frac{v_s^2 (\vec{\nabla}_x \delta)}{(1 + \delta) S} - \frac{\vec{\nabla}_x \phi}{S} + \frac{\hbar^2}{2m_\chi^2 S^3} \vec{\nabla}_x \left(\frac{\vec{\nabla}_x^2 \sqrt{1 + \delta}}{\sqrt{1 + \delta}} \right), \quad (25)$$

$$\vec{\nabla}_x^2 \phi = 4\pi G \rho_{b\chi} S^2 \delta \quad (26)$$

respectively, which have been established before in Ref. [82]. In obtaining Eq. (24), we have exploited the continuity Eq. (11) of the background. Here, we identify $\delta = \delta(\vec{r}, t) = \delta \rho_\chi(\vec{r}, t) / \rho_{b\chi}(t)$ as the density contrast. We write $v_s^2 = \partial P_{b\chi} / \partial \rho_{b\chi}$ as the square of the speed of sound supposing adiabatic fluctuations in the background BEC, can be evaluated from the equation of state (9) as

$$v_s^2 = \frac{4\pi \hbar^2 l_s \rho_{b\chi}}{m_\chi^3}. \quad (27)$$

5 Linearized perturbed equations

In the linear theory of density perturbation of structure formation, we consider tiny perturbations in comparison to zero order or unperturbed counterparts (i.e. $\delta \ll 1$, $|\vec{v}| \ll 1$ and $\phi \ll 1$). Here, in this linear regime, higher-order terms are being neglected, which means the evolution of different perturbative modes is independent of each other. In other words, the behavior of one perturbation does not significantly alter the behavior of other perturbations. This independence allows us to treat each perturbative mode separately which makes it easier to study and understand the dynamics of each mode individually [107]. Therefore linearizing the aforesaid Eqs. (24–26) by keeping up to only the first-order terms in perturbative quantities, we obtain [82]

$$\frac{\partial \delta}{\partial t} \Big|_x + \frac{1}{S} (\vec{\nabla}_x \cdot \vec{v}) = 0, \quad (28)$$

$$\left(\frac{\partial}{\partial t} \Big|_x + H \right) \vec{v} = -\frac{v_s^2 (\vec{\nabla}_x \delta)}{S} - \frac{\vec{\nabla}_x \phi}{S} + \frac{\hbar^2}{4m_\chi^2 S^3} \vec{\nabla}_x (\vec{\nabla}_x^2 \delta), \quad (29)$$

$$\vec{\nabla}_x^2 \phi = 4\pi G \rho_{b\chi} S^2 \delta \quad (30)$$

respectively. Taking the time derivative of Eq. (28), the divergence of Eq. (29) and using Eq. (30), after elimination of the term $(\vec{\nabla}_x \cdot \vec{v})$, it is now easy to combine into a single equation describing the linearized evolution equation of the density contrast of the form [82]

$$\frac{\partial^2 \delta}{\partial t^2} \Big|_x + 2H \frac{\partial \delta}{\partial t} \Big|_x = \frac{v_s^2}{S^2} \vec{\nabla}_x^2 \delta + 4\pi G \rho_{b\chi} \delta - \frac{\hbar^2}{4m_\chi^2 S^4} \vec{\nabla}_x^4 \delta. \quad (31)$$

Decomposing the perturbation in Fourier modes of the form $\delta(\vec{x}, t) = \delta_k(t) e^{i\vec{k} \cdot \vec{x}}$, and inserting into Eq. (31), we obtain for k -th perturbative mode [82]

$$\ddot{\delta}_k + 2H\dot{\delta}_k + \left(\frac{\hbar^2 k^4}{4m_\chi^2 S^4} + \frac{v_s^2 k^2}{S^2} - 4\pi G \rho_{b\chi} \right) \delta_k = 0. \quad (32)$$

The second term on the left-hand side of Eq. (32) originates due to the expansion of the Universe, and exhibits dissipation. The term containing \hbar is due to quantum pressure, while the term containing v_s arises because of the self-interaction pressure of BEC. The last term consisting of G reflects the effect of gravitational attraction. For $\hbar = 0$, we retrieve the non-quantum evolution equation first derived by Bonnor [108] and also discussed in several other texts (see Refs. [2, 105, 109] for details).

6 Solution to the evolution equation

In this section we recall the results obtained in Ref. [82] by solving Eq. (32) analytically for different regimes. Here Eq. (32) is the linearized version of the density contrast equation of BEC DM containing both quantum and self-interaction pressure. As the analytic solution to Eq. (32) is hard to achieve, we shall discuss two different cases. The first one is the non-interacting BEC, which is valid when the de-Broglie wavelengths of the condensate particles are very small compared to the typical length scales over which the density of condensate and the gravitational trapping potential fluctuate significantly. The other one is the TF approximation, which is applicable when the condensate particles are large in number and the kinetic energy of the particles is negligible [96]. Apart from these, the density contrast Eq. (32), which has been solved numerically in the general case in Ref. [66], is also reproduced as a function of the cosmic time t in Sect. 8.3. The only difference with our study is that we express the results in terms of the time t instead of the scale factor $S \propto t^{2/3}$ in Refs. [66, 82].

6.1 Case-I: Non-interacting case

In the non-interacting case $l_s = v_s = 0$, the evolution Eq. (32) reduces to

$$\ddot{\delta}_k + 2H\dot{\delta}_k + \left(\frac{\hbar^2 k^4}{4m_\chi^2 S^4} - 4\pi G \rho_{b\chi} \right) \delta_k = 0. \quad (33)$$

From Eq. (33) we can define quantum comoving Jeans wavenumber as

$$k_Q = \left(\frac{16\pi G m_\chi^2 \rho_{b\chi} S^4}{\hbar^2} \right)^{1/4}, \quad (34)$$

which is time-dependent in nature. Recalling conservation Eq. (14), we can express $k_Q = \kappa_Q S^{1/4}$ where $\kappa_Q = (16\pi G m_\chi^2 \rho_{b0\chi} S_0^3 / \hbar^2)^{1/4}$ is constant in time. The corresponding quantum comoving Jeans length is defined as $\lambda_Q = 2\pi/k_Q$ decreases with scale factor ($\propto S^{-1/4}$). Using (18), the Eq. (33) for the non-interacting case can be recast as

$$\ddot{\delta}_k + \frac{4}{3t} \dot{\delta}_k + \frac{2}{3t^2} \left(\frac{k^4}{\beta_Q^4 t^{2/3}} - 1 \right) \delta_k = 0, \quad (35)$$

where $\beta_Q^4 = S_0 \kappa_Q^4 / (2/3 H_0)^{2/3}$ is a constant. The general solution of Eq. (35) is given by

$$\begin{aligned} \delta_k(t) = & \frac{2\mathcal{C}_1}{3k^4 \left(\frac{1}{t} \right)^{2/3}} \left[\beta_Q^4 \cos \left(\frac{\sqrt{6}k^2 \left(\frac{1}{t} \right)^{1/3}}{\beta_Q^2} \right) \right. \\ & \left. - 2k^4 \left(\frac{1}{t} \right)^{2/3} \cos \left(\frac{\sqrt{6}k^2 \left(\frac{1}{t} \right)^{1/3}}{\beta_Q^2} \right) \right. \end{aligned}$$

$$\begin{aligned} & + \sqrt{6}k^2 \beta_Q^2 \left(\frac{1}{t} \right)^{1/3} \sin \left(\frac{\sqrt{6}k^2 \left(\frac{1}{t} \right)^{1/3}}{\beta_Q^2} \right) \left. \right] \\ & - \frac{15\mathcal{C}_2}{16k^4 \left(\frac{1}{t} \right)^{2/3}} \left[-\beta_Q^4 \sin \left(\frac{\sqrt{6}k^2 \left(\frac{1}{t} \right)^{1/3}}{\beta_Q^2} \right) \right. \\ & + 2k^4 \left(\frac{1}{t} \right)^{2/3} \sin \left(\frac{\sqrt{6}k^2 \left(\frac{1}{t} \right)^{1/3}}{\beta_Q^2} \right) \\ & \left. + \sqrt{6}k^2 \beta_Q^2 \left(\frac{1}{t} \right)^{1/3} \cos \left(\frac{\sqrt{6}k^2 \left(\frac{1}{t} \right)^{1/3}}{\beta_Q^2} \right) \right] \quad (36) \end{aligned}$$

where \mathcal{C}_1 and \mathcal{C}_2 are integration constants.

6.2 Case-II: TF limit

In the TF limit, as the kinetic energy term is negligible, the contribution of quantum potential can be forsaken, and the evolution Eq. (32) reduces to

$$\ddot{\delta}_k + 2H\dot{\delta}_k + \left(\frac{v_s^2 k^2}{S^2} - 4\pi G \rho_{b\chi} \right) \delta_k = 0. \quad (37)$$

Now we can define classical comoving Jeans wavenumber

$$k_J = \left(\frac{4\pi G \rho_{b\chi} S^2}{v_s^2} \right)^{1/2}, \quad (38)$$

which for the standard BEC with the speed of sound v_s in (27), takes the form

$$k_J = \left(\frac{G m_\chi^3 S^2}{l_s \hbar^2} \right)^{1/2}. \quad (39)$$

We can see that k_J is a time-dependent quantity. We denote $k_J = \kappa_J S$ with $\kappa_J = (G m_\chi^3 / l_s \hbar^2)^{1/2}$ is constant in time. The classical comoving Jeans length is defined as $\lambda_J = 2\pi/k_J$ decreases with scale factor ($\propto S^{-1}$). Using of (18) in Eq. (37) for TF limit, gives

$$\ddot{\delta}_k + \frac{4}{3t} \dot{\delta}_k + \frac{2}{3t^2} \left(\pm \frac{k^2}{\beta_J^2 t^{4/3}} - 1 \right) \delta_k = 0 \quad (40)$$

for repulsive (+ sign) and attractive (- sign) scatterings respectively. Here $\beta_J^2 = S_0^2 \kappa_J^2 / (2/3 H_0)^{4/3}$ is a constant. The general solution of Eq. (40) with $l_s > 0$ (repulsive scattering) is given by

$$\begin{aligned} \delta_k(t) = & -2^{13/8} 3^{1/8} \Gamma \left(\frac{3}{4} \right) \mathcal{D}_1 \left(\frac{k}{\beta_J} \right)^{1/4} \left(\frac{1}{t} \right)^{1/6} \\ & \mathbf{J}_{-\frac{5}{4}} \left[\sqrt{\frac{3}{2}} \left(\frac{k}{\beta_J} \right) \left(\frac{1}{t} \right)^{2/3} \right] \\ & + 2^{-3/8} 3^{1/8} \Gamma \left(\frac{9}{4} \right) \mathcal{D}_2 \left(\frac{k}{\beta_J} \right)^{1/4} \left(\frac{1}{t} \right)^{1/6} \end{aligned}$$

$$\mathbf{J}_{\frac{5}{4}} \left[\sqrt{\frac{3}{2}} \left(\frac{k}{\beta_J} \right) \left(\frac{1}{t} \right)^{2/3} \right], \quad (41)$$

where $\mathbf{J}_n[z]$ gives the Bessel function of the first kind of order n and argument z , and \mathcal{D}_1 and \mathcal{D}_2 are integration constants. On the other hand the general solution of Eq. (40) with $l_s < 0$ (attractive scattering) is given by

$$\begin{aligned} \delta_k(t) = & i 2^{13/8} 3^{1/8} \Gamma \left(\frac{3}{4} \right) \mathcal{E}_1 \left(\frac{k}{\beta_J} \right)^{1/4} \left(\frac{1}{t} \right)^{1/6} \\ & \mathbf{I}_{-\frac{5}{4}} \left[\sqrt{\frac{3}{2}} \left(\frac{k}{\beta_J} \right) \left(\frac{1}{t} \right)^{2/3} \right] \\ & + 2^{-3/8} 3^{1/8} (-1)^{3/4} \Gamma \left(\frac{9}{4} \right) \mathcal{E}_2 \left(\frac{k}{\beta_J} \right)^{1/4} \left(\frac{1}{t} \right)^{1/6} \\ & \mathbf{I}_{\frac{5}{4}} \left[\sqrt{\frac{3}{2}} \left(\frac{k}{\beta_J} \right) \left(\frac{1}{t} \right)^{2/3} \right], \end{aligned} \quad (42)$$

where $\mathbf{I}_n[z]$ gives the modified Bessel function of the first kind of order n and argument z , and \mathcal{E}_1 and \mathcal{E}_2 are integration constants. In order to investigate the evolution of density perturbation of BEC DM, we have to analyze the solutions to the density contrast equations given in Eqs. (36), (41), and (42). We have seen the solutions contain integration constants which are to be determined from initial conditions. We know the BEC DM has been converted from normal DM through a phase transition. Therefore, to get the values of integration constants in the following section, we briefly present the conversion of the BEC DM from normal DM.

7 Normal DM to BEC DM phase transition

We consider that at the early stage, the DM was in normal form with an equation of state [84, 110, 111]

$$p_\chi = c^2 \sigma_\chi^2 \rho_\chi, \quad (43)$$

where $\sigma_\chi = \sqrt{\langle \vec{v}_\chi^2 \rangle / 3c^2}$ is the 1-D velocity dispersion, and $\langle \vec{v}_\chi^2 \rangle$ is the mean squared velocity of the normal DM particles, where all the calculations are performed in the non-relativistic regime. These normal DM boson particles with mass m_χ and temperature T initiated at equilibrium and decoupled from remaining plasma at a temperature T_D in the early Universe [84, 89]. As time progressed, the Universe cooled down to T_{crit} , and the normal DM started converting to BEC through a phase transition process. Nevertheless, the transition does not happen instantaneously, rather the mixed phase coexists for a duration until all the normal DM has been transformed to condensate form. The order of the phase transition has some amount of ambiguity. In articles, [112, 113] authors commented that the phase transition is described by a spontaneous global $U(1)$ symmetry breaking with condensation factor as an order parameter. This implies a second-order

phase transition. However, It was shown in several mean-field theoretical models such as Yukalov–Yukalova, Popov, Hartree–Fock, and Many-body t-matrix have not predicted a second-order phase transition regarding normal to BEC phase transition in Ref. [114]. A rigorous study on the thermodynamic instability of a confined ideal Bose gas with a finite number of particles refers to a discontinuous phase transition as it manifests a pure mathematical singularity [115]. According to Harko [84], the first-order phase transition is the best possible way to represent the BEC dynamics.

In the context of the cosmological Bose–Einstein DM condensation process, a first-order phase transition from normal DM to BEC DM happened. By definition, during a first-order phase transition, we know that the temperature and the pressure are constants at their critical values i.e. at $T = T_{crit}$ and $P = P_{crit}$. Apart from these, enthalpy and entropy also remain conserved during the first-order phase transition. In this process, an important thermodynamic condition ‘the continuity of pressure’ must be satisfied at the transition point (T_{crit}, P_{crit}) , and this fixes the critical transition density ρ_χ^{crit} from the normal state to condensate state as [84]

$$\rho_\chi^{crit} = \frac{\sigma_\chi^2 m_\chi^3}{2\pi\hbar^2 l_s} c^2. \quad (44)$$

The DM density $\rho_\chi(t)$ started to decrease from $\rho_\chi^{crit}(T_{crit}) \equiv \rho_\chi^{nor}$ after the beginning of the phase changeover process when all the DM was in normal form, to $\rho_\chi(T_{crit}) \equiv \rho_\chi^{bec}$, corresponding to a total BEC state. The critical scale factor S_{crit} and critical redshift of transition z_{crit} can be expressed as [84]

$$S_{crit} = S_0 \left(\frac{2\pi\hbar^2 l_s \Omega_0^\chi \rho_0^{cr}}{c^2 \sigma_\chi^2 m_\chi^3} \right)^{\frac{1}{3(1+\sigma_\chi^2)}}, \quad (45)$$

and

$$z_{crit} = -1 + \left(\frac{2\pi\hbar^2 l_s \Omega_0^\chi \rho_0^{cr}}{c^2 \sigma_\chi^2 m_\chi^3} \right)^{\frac{-1}{3(1+\sigma_\chi^2)}} \quad (46)$$

respectively. Here Ω_0^χ and ρ_0^{cr} represent the DM density parameter and critical density of the Universe at present. In our present study, we have not considered the contribution of cosmological constant Λ and radiation. In this conversion process, the time taken to convert the whole normal DM to BEC is given by [84]

$$\Delta t_{cond} = \frac{2}{3H_0\sqrt{\Omega_{tr}}} [(1+r)^{-1/2} - 1], \quad (47)$$

where $r = \frac{\rho_\chi^{bec} - \rho_\chi^{nor}}{\rho_\chi^{nor} + P_{crit}/c^2}$ is a number. In general $r < 0$, and $r \in (-1, 0)$. The term Ω_{tr} in the last expression (47) can be identified as

$$\Omega_{tr} = \frac{\Omega_0^b}{(S_{crit}/S_0)^3} + \Omega_\chi^{nor}, \quad (48)$$

where Ω_0^b is the baryonic density parameter at present time and we have identified $\Omega_\chi^{nor} = \rho_\chi^{nor}/\rho_0^{cr}$. In [90], it was shown that cosmic BEC is formed when the boson satisfies the mass constraint $m_\chi < 1.87$ eV. Taking $m_\chi \approx 0.553048$ eV, $r = -0.910646$ within the limitations, assuming standard values $l_s = 10^{-10}$ cm and $\sigma_\chi^2 = 3 \times 10^{-6}$, we get $z_{crit} \approx 1200$ and $\Delta t_{cond} \approx 10^6$ years from Eqs. (46) and (47) respectively. Here we have also used the most accepted values of the quantities $H_0 = 70 \text{ km.sec}^{-1} \text{Mpc}^{-1} = 2.27 \times 10^{-18} \text{ sec}^{-1}$, $\rho_0^{cr} = 9.24 \times 10^{-30} \text{ g cm}^{-3}$, $\Omega_0^\chi \approx 0.228$, and $\Omega_0^b = 0.045$ [84, 116]. From the time-redshift relation [117]

$$t \approx \frac{28}{1 + (1 + z)^2} \text{ Gyrs}, \quad (49)$$

we get the time $t_{crit} \approx 6.12179 \times 10^{11}$ s corresponding to critical redshift $z_{crit} \approx 1200$, indicating the beginning of phase transition process. Therefore the post-condensation phase started at approximately $t_{post} = (t_{crit} + \Delta t_{cond}) \approx 3.21482 \times 10^{13}$ s after the big bang ($t_{bb} = 0$). The corresponding redshift value is $z_{post} \approx 164.728$. In Sects. 3, 4, and 5, regarding the derivation of the density contrast equation of BEC DM, we have followed an approach similar to that in non-relativistic Newtonian consideration. In Sect. 6, we have obtained the solutions for both the non-interacting case and the TF limit. In this context, it is worth introducing the fact that in the Newtonian approach, we can only consider the wavelength λ of perturbations to be well inside the Hubble radius d_H in which the General Relativistic effect due to space-time curvature is negligible. At $z > 1000$, the modes of the perturbation enter the Hubble radius. So their wavelengths are smaller than the Hubble radius only at $z \lesssim 1000$ [118]. Just now we have found out that BE condensate phase has been completed at around a redshift 164.728, and we analyze the evolution feature of the density contrast of BEC DM from $z_{post} \approx 164.728$ ($t_{post} \approx 3.21428 \times 10^{13}$ s) upto present epoch $z_0 = 0$ ($t_0 \approx 14$ Gyrs $\approx 4.41504 \times 10^{17}$ s). Thus, we can fully rely on the non-relativistic Newtonian approach.

8 Results and discussions

Here, in this present section, in order to explain the evolutionary behavior of density contrast of BEC DM in terms of cosmic time, we rederive the results of Ref. [66] presented in terms of the scale factor. In Sect. 6, we have presented the general solutions of the density contrast equation of BEC DM for Case I: Non-interacting BEC and Case II: TF limit. In order to get an idea of the nature of the solutions, now we discuss both cases, particularly analyzing the temporal behavior of the solutions. In addition, we also discuss self-interacting BEC for both repulsive and attractive scatterings

beyond the TF approximation where none of the pressures are being ignored. In that case, we could hardly solve the evolution equation analytically but a numerical analysis is possible and presented considering proper initial conditions.

8.1 Evolution of density contrast of the non-interacting BEC

In the non-interacting case, the force term that originates from quantum pressure is important. Here we can point out two regimes depending on two extreme conditions. At first, we consider the regime where the quantum pressure dominates highly over the gravity i.e. $k/\beta_Q >> t^{1/6}$, In this case, Eq. (35) reduces to

$$\ddot{\delta}_k + \frac{4}{3t}\dot{\delta}_k + \frac{2}{3t^2} \left(\frac{k^4}{\beta_Q^4 t^{2/3}} \right) \delta_k = 0, \quad (50)$$

exhibits a fully oscillatory solution of the form

$$\delta_k(t) = \mathcal{A}_1 \cos \left[\sqrt{6} \left(\frac{k}{\beta_Q} \right)^2 \left(\frac{1}{t} \right)^{1/3} \right] - \mathcal{A}_2 \sin \left[\sqrt{6} \left(\frac{k}{\beta_Q} \right)^2 \left(\frac{1}{t} \right)^{1/3} \right]. \quad (51)$$

Here $\mathcal{A}_1, \mathcal{A}_2$ are integration constants. From the analysis of Jeans instability, we can say that the perturbation wavelength is smaller than the quantum Jeans length ($\lambda << \lambda_Q$) in this regime. Therefore, the density contrast cannot grow. This is obvious because of the dominating effect of quantum pressure over gravity. Secondly, we consider the case $k/\beta_Q << t^{1/6}$, the Eq. (35) modifies to

$$\ddot{\delta}_k + \frac{4}{3t}\dot{\delta}_k - \frac{2}{3t^2} \delta_k = 0. \quad (52)$$

In comparison to the previous case, here Eq. (52) gives a general solution of the form

$$\delta_k(t) = \mathcal{A}_3 t^{2/3} + \mathcal{A}_4 t^{-1}, \quad (53)$$

containing growing and decaying mode as the gravitational collapse suppresses the quantum pressure. Here \mathcal{A}_3 and \mathcal{A}_4 are integration constants. In this regime, the perturbation wavelength is greater than the quantum Jeans length ($\lambda >> \lambda_Q$), and the density contrast grows/decays according to Jeans's theory. This case is similar to the CDM case or pressureless matter-dominated Universe. Thus it is clear from the Eq. (35) that the quantum pressure dominates at time $t << (k/\beta_Q)^6$ and the perturbation will oscillate, and at time $t >> (k/\beta_Q)^6$ gravity takes over and the perturbation grows/decays.

So far, in the above, from Jeans's theoretic point of view we have analytically analyzed the evolution of density contrast of BEC DM by solving Eq. (35) in two extreme conditions. Particularly, from the above analysis, it is to be noted

that the effect of quantum potential is negligible on a large scale, but one can recover the CDM model within the framework of classical hydrodynamics. On a small scale, we see the quantum Jeans length λ_Q gives a sharp cut-off, below which growth is impossible.

In order to visualize the temporal behavior of evolution for the period from the beginning of the post-condensation (t_{post}) to present time (t_0), we now concentrate on the general solution (36) of Eq. (35) for plotting. If we take the ratio $k/\beta_Q \geq t_0^{1/6} \approx 872.625 \text{ sec}^{1/6}$, the perturbation would show pure oscillatory behavior from the beginning of post-BEC phase t_{post} up to the present time t_0 (see Fig. 1a). Next, for the ratio $k/\beta_Q \leq t_{post}^{1/6} \approx 178.317 \text{ sec}^{1/6}$, there would be no oscillation, rather the solution grows/decays from the beginning t_{post} up to the present time t_0 (see Fig. 1b). In the intermediate regime $t_{post}^{1/6} \approx 178.317 \text{ sec}^{1/6} < k/\beta_Q < t_0^{1/6} \approx 872.625 \text{ sec}^{1/6}$, the density contrast first shows pure oscillations until a critical time $t_{cr1} \sim (k/\beta_Q)^6$, then grows/decays. This is shown in Fig. 1c. Here we should note that the temporal evolution of density contrast shown in the three cases in Fig. 1 in our present study corresponds to the results presented in Figs. 2, 3, and 4 of Ref. [66] where evolutionary behavior is shown in terms of the scale factor.

From the above analysis, we can see from Fig. 1a that the amplitude of the oscillation is constant throughout the evolution in the non-interacting regime, but is not manifested from the solution (36). It would be transparent if we recast the solution in terms of Bessel functions as

$$\delta_k(t) \propto \left(\frac{1}{t}\right)^{1/6} \mathbf{J}_{\pm \frac{5}{2}} \left[\sqrt{6} \left(\frac{k}{\beta_Q}\right)^2 \left(\frac{1}{t}\right)^{1/3} \right], \quad (54)$$

which is also given in Refs. [66, 82] but expressed in terms of scale factor. Expanding the Bessel function in (54) asymptotically for large arguments ($t \ll (k/\beta_Q)^6$) [119], we write

$$\delta_k(t) = \mathcal{C}'_1 \sin \left[\sqrt{6} \left(\frac{k}{\beta_Q}\right)^2 \left(\frac{1}{t}\right)^{1/3} \right] + \mathcal{C}'_2 \cos \left[\sqrt{6} \left(\frac{k}{\beta_Q}\right)^2 \left(\frac{1}{t}\right)^{1/3} \right], \quad (55)$$

where \mathcal{C}'_1 and \mathcal{C}'_2 are constants. As expected the solution (55) is exactly the same as that in (51) with $\mathcal{C}'_1 = -\mathcal{A}_2$ and $\mathcal{C}'_2 = \mathcal{A}_1$, is also presented in Ref. [66] keeping scale factor as independent variable in place of time. From (55), we notice the amplitudes are independent of time t . Therefore the oscillation with constant amplitude is properly justified. In this context, it is to be noted that the two regimes (oscillation and growth) and the fact that the amplitude of the oscillation is constant in the non-interacting regime have been discussed in detail in Ref. [66]

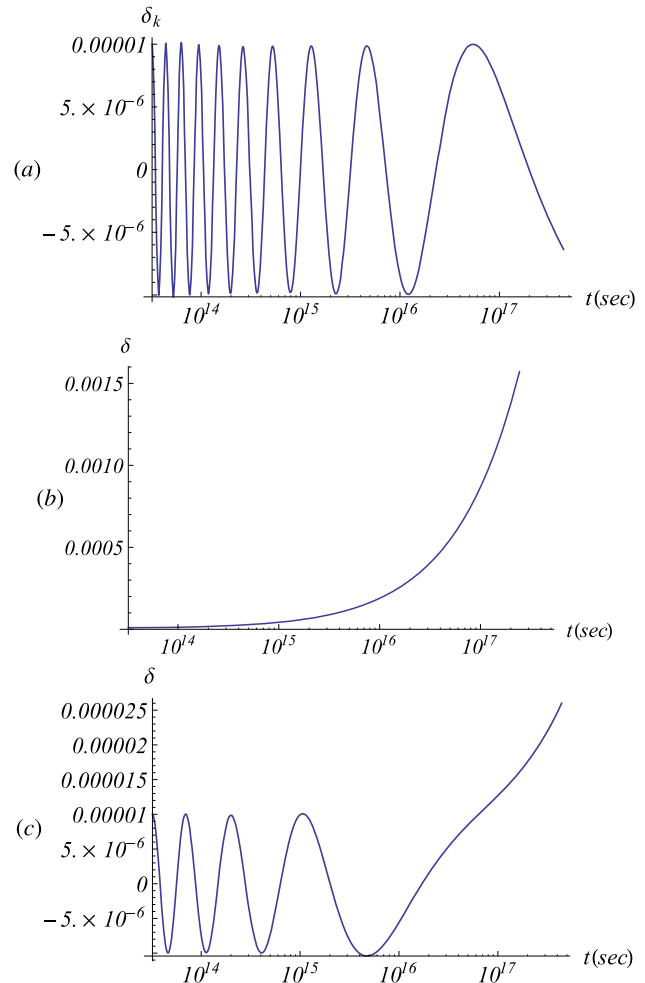


Fig. 1 Log-linear plots of the evolution of density contrast δ_k of Eq. (35) as a function of cosmic time t (secs) for the non-interacting cases: (a) $k/\beta_Q = 900 \text{ sec}^{1/6}$, (b) $k/\beta_Q = 150 \text{ sec}^{1/6}$, (c) $k/\beta_Q = 600 \text{ sec}^{1/6}$, where the perturbation oscillates until a critical time $t_{cr1} \sim 600^6 \text{ sec} \approx 4.67 \times 10^{16} \text{ sec}$, and then grows. [Initial conditions: $\delta_k(3.21482 \times 10^{13} \text{ sec}) = 10^{-5}$, $\dot{\delta}_k(3.21482 \times 10^{13} \text{ sec}) = 0$]

8.2 Evolution of density contrast in the TF limit

In the above subsection, we have discussed the evolution of density contrast of BEC DM for the non-interacting case. Compared to the previous case, in the TF limit (neglecting the quantum pressure term), we shall now discuss the same but for two different cases. Case I: Repulsive scattering ($l_s > 0$), and Case II: Attractive scattering ($l_s < 0$).

8.2.1 Case I: Repulsive scattering ($l_s > 0$):

In the TF limit, the self-interaction term outplays the quantum pressure term. Similar to the previous case study, here also we can identify two regimes depending on two extreme conditions for positive scattering length ($l_s > 0$). At first, we

consider the regime where the self-interaction pressure dominates highly over the gravity i.e. $k/\beta_J \gg t^{2/3}$, the density contrast Eq. (40) reduces to

$$\ddot{\delta}_k + \frac{4}{3t}\dot{\delta}_k + \frac{2}{3t^2} \left(\frac{k^2}{\beta_J^2 t^{4/3}} \right) \delta_k = 0. \quad (56)$$

The solution of Eq. (56) is given by

$$\delta_k(t) = 2^{-3/8} 3^{1/8} \Gamma \left(\frac{3}{4} \right) \mathcal{B}_1 \left(\frac{k}{\beta_J} \right)^{1/4} \left(\frac{1}{t} \right)^{1/6} J_{-\frac{1}{4}} \left[\sqrt{\frac{3}{2}} \left(\frac{k}{\beta_J} \right) \left(\frac{1}{t} \right)^{2/3} \right] + 2^{-3/8} 3^{1/8} \Gamma \left(\frac{5}{4} \right) \mathcal{B}_2 \left(\frac{k}{\beta_J} \right)^{1/4} \left(\frac{1}{t} \right)^{1/6} J_{\frac{1}{4}} \left[\sqrt{\frac{3}{2}} \left(\frac{k}{\beta_J} \right) \left(\frac{1}{t} \right)^{2/3} \right], \quad (57)$$

where \mathcal{B}_1 and \mathcal{B}_2 are integration constants. It shows pure oscillatory behavior because here self-interaction pressure highly dominates over gravity. In other words, the perturbation wavelength is much smaller than classical Jeans length ($\lambda \ll \lambda_J$) in this regime, and obviously, the perturbation cannot grow.

For the second case, when the ratio $k/\beta_J \ll t^{2/3}$, the density contrast equation in (40) reduces to (52) with solution (53). Here in this regime, the perturbation wavelength is much greater than the classical Jeans length ($\lambda > \lambda_J$), and Jeans's instability theory confirms the growth/decay of the density contrast. The above analysis concludes that the self-interaction pressure dominates at time $t \ll (k/\beta_J)^{3/2}$, the perturbation will oscillate, and at time $t \gg (k/\beta_J)^{3/2}$ gravity rules over, the perturbation grows/decays.

Until now, in the above, we have investigated analytically the evolution of density perturbation of condensed DM by solving Eq. (40) in two extreme conditions for positive scattering. In order to understand the temporal evolutionary picture of density contrast, we now pay attention to the general solution (41) of Eq. (40) for the positive scattering case and plot it from the post-condensation phase to the present epoch. Now, if we take the ratio $k/\beta_J \geq t_0^{2/3} \approx 5.798 \times 10^{11} \text{ sec}^{2/3}$, the density perturbation would display pure oscillatory behavior from t_{post} to t_0 (see Fig. 2a). For the ratio $k/\beta_J \leq t_{\text{post}}^{2/3} \approx 1.011 \times 10^9 \text{ sec}^{2/3}$, the density contrast grows/decays for the entire regime (see Fig. 2b). In the intermediate regime $t_{\text{post}}^{2/3} \approx 1.011 \times 10^9 \text{ sec}^{2/3} < k/\beta_J < t_0^{2/3} = 5.798 \times 10^{11} \text{ sec}^{2/3}$, the density contrast first shows pure oscillatory solutions until a critical time $t_{\text{cr2}} \sim (k/\beta_J)^{3/2}$ and after that it grows/decays (see Fig. 2c). Here it is also to be noted that the time evolution of density contrast shown in the three cases in Fig. 2 in our results corresponds to the plots presented in Figs. 3, 5, and 6 of Ref.

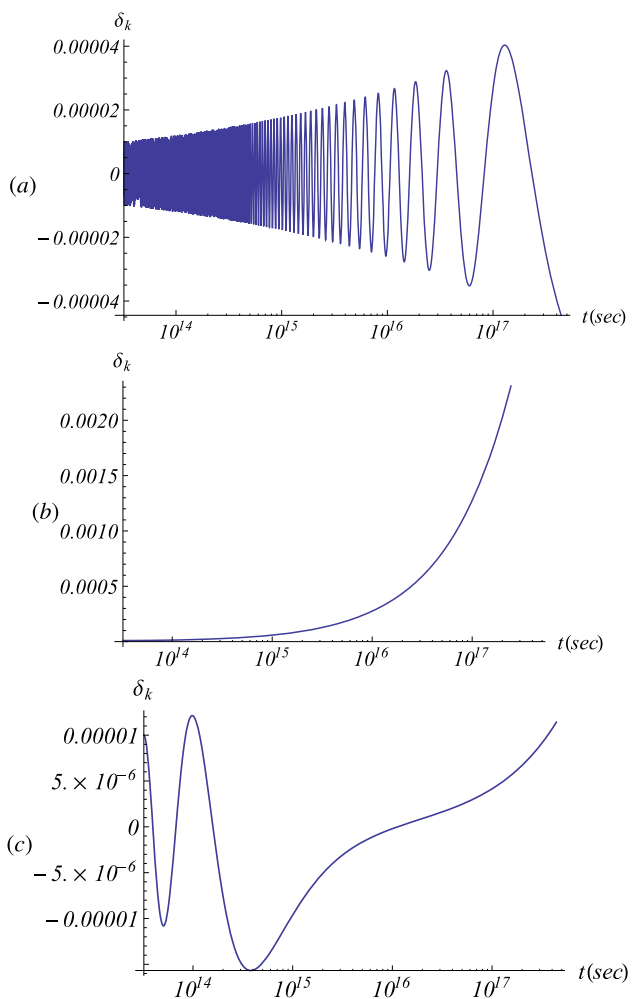


Fig. 2 Log-linear plots of the evolution of density contrast δ_k of Eq. (40) as a function of cosmic time t (sec) with positive scattering for the TF limit cases: (a) $k/\beta_J = 10^{12} \text{ sec}^{2/3}$, (b) $k/\beta_J = 10^8 \text{ sec}^{2/3}$, (c) $k/\beta_J = 10^{10} \text{ sec}^{2/3}$, where the perturbation oscillates until a critical time $t_{\text{cr2}} \sim (10^{10})^{3/2} \text{ sec} \approx 10^{15} \text{ sec}$, and then grows. [Initial conditions: $\delta_k(3.21482 \times 10^{13} \text{ sec}) = 10^{-5}$, $\dot{\delta}_k(3.21482 \times 10^{13} \text{ sec}) = 0$]

[66] where evolutionary behavior in terms of the scale factor is considered.

From the above analysis in the TF regime, we observe from Fig. 2a that the oscillation amplitude is increasing as time progresses. It is hard to understand this fact from the solution (41). To visualize the growing amplitude of the oscillatory solution, we expand the Bessel functions asymptotically for large arguments ($t \ll (k/(\beta_J)^{3/2})$ [119], and write (41) as

$$\delta_k(t) = \mathcal{D}'_1 t^{1/6} \cos \left[\sqrt{\frac{3}{2}} \left(\frac{k}{\beta_J} \right) \left(\frac{1}{t} \right)^{2/3} - \frac{7}{8}\pi \right] + \mathcal{D}'_2 t^{1/6} \cos \left[\sqrt{\frac{3}{2}} \left(\frac{k}{\beta_J} \right) \left(\frac{1}{t} \right)^{2/3} + \frac{3}{8}\pi \right], \quad (58)$$

where \mathcal{D}'_1 and \mathcal{D}'_2 are constants, which is expressed in Ref. [66] as a function of scale factor. From (58), the growth of

oscillation amplitude ($\propto t^{1/6}$) is now well understood. As before, here the two regimes (oscillation and growth) and the fact that the amplitude of the oscillation increases in the TF regime have been discussed in detail also in Ref. [66].

8.2.2 Case II: Attractive scattering ($l_s < 0$):

In the TF approximation when the scattering length is negative ($l_s < 0$), there will be no opposing pressure force to counteract gravitational attraction, rather the pressure due to negative scattering length would help gravitational collapse. So (42) always shows a growing or decaying mode of solution for the density contrast of BEC DM for any value of wavenumber k . For very small k (large scale) the density contrast solution behaves as CDM solution (53). For large k (small scale), the BEC DM density contrast drastically grows from the beginning because the additive BEC interaction pressure force due to attractive scattering along with gravity force helps gravitational instability, resulting in furious exponential collapse to form the BEC structure. The initial rapid exponential growth can be understood by expanding the modified Bessel functions in (42) asymptotically for large arguments [120] i.e. for $t \ll (k/(\beta_J)^{3/2})$, and write (42) as

$$\delta_k \propto t^{1/6} \exp \sqrt{\frac{3}{2}} \left(\frac{k}{\beta_J} \right) \left(\frac{1}{t} \right)^{2/3}. \quad (59)$$

This fact is shown diagrammatically in Fig. 5, denoted by P_1 for the TF limit. A similar equivalent solution of Eq. (59) is studied in terms of scale factor and is given in Eq. (67) of Ref. [82]. In this context we should also note a similar discussion on the rapid exponential growth of density contrast with respect to scale factor is shown in Fig. 10 of Ref. [66].

8.3 Evolution of density contrast of self-interacting BEC beyond the TF limit

In the previous two subsections, we have discussed the evolution of density contrast of BEC DM by solving the density contrast equation analytically for the non-interacting BEC and the BEC in the TF limit respectively. Here we keep both pressure terms simultaneously in the density contrast equation with a view to studying the evolutionary nature of the density contrast of BEC DM. As the system is very complicated, we have faced difficulties in finding analytical solutions. So in the presence of both the pressure terms, we analyze the system by solving it numerically. More specifically, the solutions are analyzed qualitatively in the time domain by means of scaling arguments in order to understand the evolution of the perturbation which was first discussed in the same terms in Ref. [66] but in the domain of scale factor. In the presence of quantum pressure term, we study the density contrast equation of BEC DM for the following two cases.

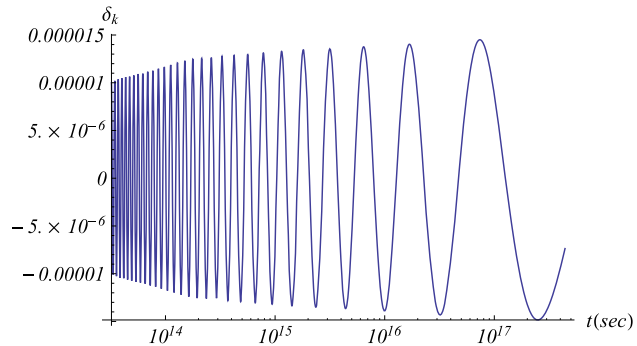


Fig. 3 Log-linear numerical plot of the evolution of density contrast δ_k of Eq. (60) as a function of cosmic time t (sec) with positive scattering length beyond the TF limit: $k/\beta_Q = 1300 \text{ sec}^{1/6}$, and $\beta_Q/\beta_J = 7.69231 \times 10^7 \text{ sec}^{1/2}$. [Initial conditions: $\delta_k(3.21482 \times 10^{13} \text{ sec}) = 10^{-5}$, $\dot{\delta}_k(3.21482 \times 10^{13} \text{ sec}) = 0$]

Case I: Repulsive scattering ($l_s > 0$), and Case II: Attractive scattering ($l_s < 0$).

8.3.1 Case I: Repulsive scattering ($l_s > 0$):

For the repulsive or positive scattering ($l_s > 0$) with the quantum pressure term, the evolution equation for BEC DM can be written from Eqs. (35), and (40) as

$$\ddot{\delta}_k + \frac{4}{3t} \dot{\delta}_k + \frac{2}{3t^2} \left(\frac{k^4}{\beta_Q^4 t^{2/3}} + \frac{k^2}{\beta_J^2 t^{4/3}} - 1 \right) \delta_k = 0. \quad (60)$$

Equation (60) corresponds to Eq. (54) as well as Eq. (132) of Refs. [82] and [66] respectively, except in our case it is expressed in time instead of the scale factor. From Eq. (60), we can see that both the quantum and self-interaction pressure collectively confront the gravitational collapse. The self-interaction term rules over the quantum term when time $t \ll (\beta_Q^4/k^2\beta_J^2)^{3/2}$ for a given wavenumber k and the system enters the TF regime. For a given wavenumber k at time $t \gg (\beta_Q^4/k^2\beta_J^2)^{3/2}$ the quantum term influences more than the self-interaction term, and the system enters in the non-interacting regime. This can be visualized by solving Eq. (60) numerically. For that, we took typical values of the ratios $k/\beta_Q = 1300 \text{ sec}^{1/6}$ and $\beta_Q/\beta_J = 7.69231 \times 10^7 \text{ sec}^{1/2}$, and plot the solution (see Fig. 3). We see for this value of k , the system enters TF regime at time $t \ll 2.07 \times 10^{14} \text{ sec}$, and non-interacting regime at time $t \gg 2.07 \times 10^{14} \text{ sec}$. These two regimes can be identified easily from the graphical analysis presented separately in Sects. 8.1 and 8.2 by observing the nature of the perturbation. We note that, whenever the perturbation oscillates with constant amplitude, the system is in a non-interacting regime and whenever there is a growing oscillation, the system is in the TF regime.

So far in the above, we have analyzed the evolution of the density contrast for the BEC DM for the positive self-interaction beyond the TF limit. Particularly, we have tried

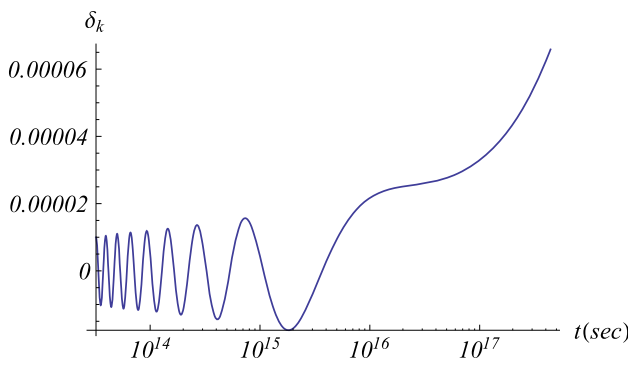


Fig. 4 Log-linear numerical plot of the evolution of density contrast δ_k of Eq. (60) as a function of cosmic time t (sec) with positive scattering length beyond the TF limit: $k/\beta_Q = 500 \text{ sec}^{1/6}$, and $\beta_Q/\beta_J = 7.93651 \times 10^7 \text{ sec}^{1/2}$. Here the perturbation oscillates until a critical time $t_{cr3} \approx 2.33782 \times 10^{16} \text{ sec}$, and then grows. [Initial conditions: $\delta_k(3.21482 \times 10^{13} \text{ sec}) = 10^{-5}$, $\dot{\delta}_k(3.21482 \times 10^{13} \text{ sec}) = 0$]

to understand the oscillatory behavior of evolution as a function of cosmic time and identified the regimes of domination of self-interaction pressure (i.e. the TF regime) and quantum pressure (i.e. the non-interacting regime). In the following, to analyze the competition between pressure terms and gravity, in the formation of BEC DM structures, we solved Eq. (60) numerically with ratios $k/\beta_Q = 500 \text{ sec}^{1/6}$, and $\beta_Q/\beta_J = 7.93651 \times 10^7 \text{ sec}^{1/2}$. The temporal evolution of the density contrast of BEC DM is depicted in Fig. 4. An interesting outcome is visualized that before a critical time, the total pressure overwhelmingly dominates gravity resulting in oscillations, whereas just after that critical time the effect of both pressures starts to weaken and gravity promotes growth. Here we find the critical time $t_{cr3} \approx 2.33782 \times 10^{16} \text{ sec}$ by equating the terms in the parentheses of Eq. (60) to zero for the aforementioned values of the ratios. An analogous numerical study for scalar-field DM has been presented in Ref. [66] taking consideration of scale factor as an independent variable in position of time. Figures 3 and 4 correspond to Figs. 7 and 8 of Ref. [66].

8.3.2 Case II: Attractive scattering ($l_s < 0$):

In the presence of quantum pressure, and attractive self-interaction ($l_s < 0$), the density contrast equation for BEC DM can be written from Eqs. (35), and (40) as

$$\ddot{\delta}_k + \frac{4}{3t}\dot{\delta}_k + \frac{2}{3t^2} \left(\frac{k^4}{\beta_Q^4 t^{2/3}} - \frac{k^2}{\beta_J^2 t^{4/3}} - 1 \right) \delta_k = 0. \quad (61)$$

Equation (61), which corresponds to Eq. (143) in Ref. [66] except for cosmic time t as an independent variable tells that the self-interaction pressure term helps gravity but the quantum pressure term opposes the collapse. So, there is no doubt that when quantum pressure is very small (or negligi-

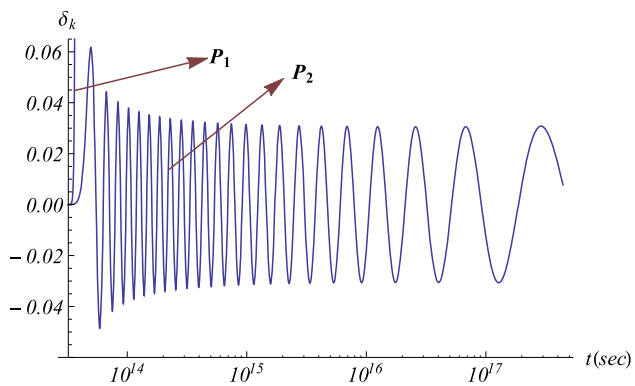


Fig. 5 Log-linear numerical plots of the evolution of density contrast δ_k of Eq. (61) as a function of cosmic time t (sec) with negative scattering length for the TF limit (Plot- P_1), and for the self-interacting BEC beyond the TF limit (Plot- P_2): $k/\beta_J = 10^{11} \text{ sec}^{2/3}$, and $\beta_Q/\beta_J = 5.98802 \times 10^7 \text{ sec}^{1/2}$. [Initial conditions: $\delta_k(3.21482 \times 10^{13} \text{ sec}) = 10^{-5}$, $\dot{\delta}_k(3.21482 \times 10^{13} \text{ sec}) = 0$]

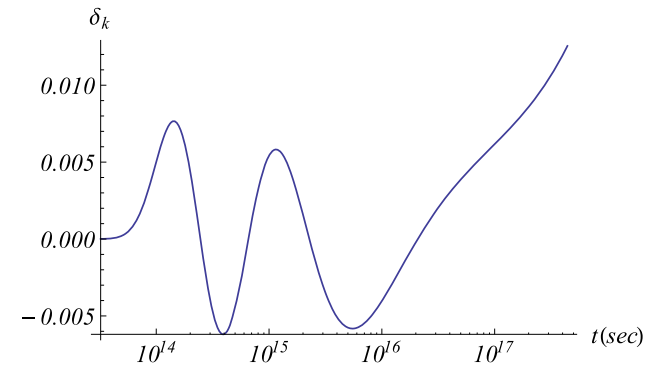


Fig. 6 Log-Linear numerical plot of density contrast δ_k of Eq. (61) as a function of cosmic time t (sec) with negative scattering length beyond the TF limit: $k/\beta_Q = 620 \text{ sec}^{1/6}$, and $\beta_Q/\beta_J = 3.33333 \times 10^7 \text{ sec}^{1/2}$. Here the perturbation grows upto a critical time $t_{cr4} \approx 1.00044 \times 10^{14} \text{ sec}$, then oscillates until another critical time $t_{cr5} \approx 5.55622 \times 10^{16} \text{ sec}$, and then grows again. [Initial conditions: $\delta_k(3.21482 \times 10^{13} \text{ sec}) = 10^{-5}$, $\dot{\delta}_k(3.21482 \times 10^{13} \text{ sec}) = 0$]

ble), density contrast grows rapidly but when the quantum term is much greater than the self-interacting term at time $t \gg (\beta_Q^4/k^2\beta_J^2)^{3/2}$, prevailing non-interacting regime for a particular wavenumber k , and the perturbation starts oscillating with a constant amplitude similar to the case study presented in Sect. 8.1. We see from the numerical plot (see Fig. 5- P_2) for a typical value of wavenumber $k/\beta_J = 10^{11} \text{ sec}^{2/3}$ and $\beta_Q/\beta_J = 5.98802 \times 10^7 \text{ sec}^{1/2}$, the density perturbation oscillates at time $t \gg 4.61 \times 10^{13} \text{ sec}$. In the initial stage ($t \ll 4.61 \times 10^{13} \text{ sec}$) when the attractive self-interacting pressure dominates together with gravity, the density contrast grows, but as soon as the quantum pressure becomes dominant at a small scale (large k), it rapidly brings stability to the system through an oscillatory solution by stopping the growth. For scalar-field DM, similar kinds of phenomena are also discussed and plotted in Fig. 10 of Ref. [66].

So far, we have attempted to get an idea of the nature of the evolution of the density contrast by identifying the regime of the supremacy of the repulsive quantum pressure (i.e. the non-interacting regime). On the contrary, presented in positive self-interaction beyond the TF limit case, negative interaction pressure always assists existing gravity resulting in a rapid exponential growth when both effects overcome the quantum pressure. Thus, negative self-interaction confirms the non-existence of oscillations in the TF regime. In the following, the contest between the quantum pressure's effect, and collective effects of gravity and attractive self-interaction pressure is analyzed. For this, we solve Eq. (61) numerically for the ratios $k/\beta_Q = 620 \text{ sec}^{1/6}$, and $\beta_Q/\beta_J = 3.33333 \times 10^7 \text{ sec}^{1/2}$, which is portrayed in Fig. 6. Interestingly, we see from the plot, that the perturbation grows up to a critical time $t_{cr4} \approx 1.00044 \times 10^{14} \text{ sec}$, then oscillates until another critical time $t_{cr5} \approx 5.55622 \times 10^{16} \text{ sec}$, and then grows again. In between two critical times, the repulsive effect of the quantum term subjugates the other attractive terms, generating oscillatory perturbations. Except this, at other times the predominating attractive terms induce growth in the density contrast leading to the formation of structures.

9 Conclusion

We have discussed early in this text that the normal DM in equilibrium decoupled from the remaining plasma state at a temperature T_D . With the expansion of the Universe, the DM underwent a first-order phase transition below the critical temperature T_{cr} and converted into the BEC form, so-called the BEC DM. Here, we have studied the evolution of cosmological density perturbation of BEC DM considering linear perturbation theory, where small cosmological perturbations are taken with respect to a homogeneous and isotropic background Universe, and the dynamics of evolution of the background Universe follows the E-dS rule. In deriving the model equation for the density contrast of BEC DM, we have assumed a gravitationally trapped BEC, governed by the GPP system. In this consideration, the Euler equation automatically produces a quantum potential term V_Q that arises due to Heisenberg's uncertainty principle. In our study, as we have assumed DM is non-relativistic and perturbation wavelengths stay well inside the horizon, the Newtonian approach is well suited. In particular, we have investigated the temporal evolution of the density contrast of the BEC DM by solving the evolution equation analytically for the non-interacting case and in the TF limit for the period from the time of post-condensation phase t_{post} to present time t_0 . During this phase, we have also studied the equation numerically without applying any approximation i.e. for the self-interacting BEC beyond the TF limit. In the figures, we have shown log-linear plots of density contrast

versus cosmic time for different scales. Among them, only the growing solutions lead to structure formation. In this article, we worked with typical numerical values of BEC parameters $(m_\chi, l_s, \sigma^2, r)$, which are very uncertain. A small change in the values of the BEC parameters could lead to drastic changes in the time scales $(t_{crit}, \Delta t_{cond}, t_{post})$. Therefore, from these theoretical predictions of the BEC DM model, one cannot match with cosmological observations until fixing the BEC parameters accurately.

The outcomes of our study are summarized as follows:

1. In the Sect. 8.1, we consider the non-interacting BEC where pressure due to self-interaction is neglected. We see for relatively large scales (small k), perturbations show oscillations with constant amplitude (see Fig. 1a), whereas perturbations grow for relatively large scales (small k) (see Fig. 1). In the intermediate scales, the density contrast oscillates up to a critical time and then grows (see Fig. 1c). Hence, the repulsive effect due to quantum potential assures that the system chooses to be stable on the small scales (order $\sim \lambda_Q$), which in turn restrain the formation of structures at small scales. Here, we also note that the growing solutions reduce to the CDM solutions when the quantum pressure is almost negligible (see (53)).
2. In the next Sect. 8.2, we studied BEC in TF limit with both positive and negative scatterings. For positive scattering, we observe perturbations display stable oscillatory solutions with increasing amplitudes for large scales (see Fig. 2a), growing solutions for small scales (see Fig. 2b), and in the intermediate scales, perturbations first show oscillations until a critical time and then grows (see Fig. 2c). Thus, like quantum pressure, repulsive self-interaction also provides a small-scale cut-off λ_J , below which the structure formation is impossible. In this context, we also mention that just like the non-interacting case the growing solutions follow CDM solutions when the self-interacting BEC pressure is inconsiderable.
3. In the same subsection, we see for the negative scattering in the TF limit, that perturbations show always growing solutions for any scale, particularly exponential growth at the initial stage (see Fig. 5- P_1). This all-time growth of density contrast is because there is no positive pressure to counter the collapse. As the negative self-interacting pressure helps gravity to collapse, the growth rate is quite high in comparison to CDM.
4. Afterwards, we discussed self-interacting BEC with positive scattering beyond the TF approximation in Sect. 8.3. From the oscillatory behavior shown in Fig. 3, we notice that at the earlier stage, the system was in the TF regime, and at the later stage the system entered the non-interacting regime. The numerical plot of Fig. 4 informs

the oscillatory nature of density contrast until a critical time, followed by growth.

5. Finally, in the same subsection self-interacting BEC with negative scattering beyond the TF approximation is analyzed. Figure 5- P_2 indicates that there is an initial high growth in perturbations due to poor quantum pressure resistance, followed by oscillations due to the dominance of quantum pressure after a critical time. In Fig. 6 similar type of plot is shown but here we notice two critical times where the nature of perturbations change.

Now we would like to recall two important problems related to the cosmological structure formation study in the Λ CDM model. The first one is the ‘cusp-core problem’ [45, 48, 49, 121], which states that in cosmological N -body CDM simulations, the isothermal density distribution of DM halos diverges and leads to a cuspy profile near the center of the structures. However, observations show a nearly flat density core with finite value contradicting the cuspy nature of the core predicted in the CDM simulations [44, 47, 122, 123]. The other problem is the ‘missing satellite problem’ [45, 62, 121]. Here N -body CDM simulations predict an excessive amount of subhalos in the galactic halo, though such a large number of satellite galaxies do not exist in the Universe [44, 60, 61, 123]. The aforesaid two problems, that arise in the Λ CDM model are due to the non-existence of the Jeans length concept, and consequently, all the scales are unstable. Thus, the density contrast of pressureless CDM will grow due to gravitational instability and eventually collapse to form both small and large-scale structures. Though the Λ CDM model is extraordinarily successful in explaining large-scale structure formation [124], it fails to explain the underabundance of small-scale structures like dwarf galaxies in the Universe as stated in the ‘missing satellite problem’. Nevertheless, we see from our study in this article the BEC DM model provides a finite small-scale cut-off (order $\sim \lambda_Q$) due to quantum effects below which structures cannot form. Hence, the repulsive effect due to quantum potential assures the system chooses to be stable on the small scales, which in turn is able to solve the so-called ‘missing satellite problem’. On the other hand, pressure due to quantum potential and self-interaction pressure (for repulsive scattering) of BEC DM obstruct gravitational collapse at the small scales, and give rise to flat-density cores in lieu of cusps, solving the ‘cusp-core problem’. We also observe that only attractive self-interaction approves the structure formation at the early stage of the Universe. This overabundance of small-scale structures at the early epoch contradicts the observations so far. For the same reason, the Λ CDM model has also been criticized due to the overabundance of substructures. Apart from that, for $l_s < 0$, equilibrium configurations of realistic DM halos cannot be obtained above a maximum mass $M_{max} = 1.012\hbar/\sqrt{Gm_\chi|l_s|}$, which is ridiculously small

(order of the Planck mass M_p) unless the mass of each boson m_χ and scattering length l_s are extremely small (e.g. QCD axions and ultralight bosons [65, 125, 126]) [94, 95]. Therefore, the consideration of only negative scattering in the context of structure formation looks infertile. Although the concept of negative pressure due to attractive boson-boson interaction helps us to explain the present accelerated Universe without assuming any other form of DE [87]. Furthermore, for the very small negative scattering length, typically for $|l_s| << 10^{-60}$ fm, if the effect of quantum pressure is not avoided, it can stabilize the modes of perturbation at small scales preventing overabundance of small scale structures like satellite galaxies, but at large scales, growth in density contrast enhances large scale structure formation just like CDM [66].

In summary, in our study we have taken into consideration the normal to BEC cosmological phase transition process in order to study the cosmological density perturbation of BEC DM. Rederiving the evolution equation of density contrast of BEC DM we found analytical solutions in terms of cosmic time rather than scale factor for both non-interacting and TF limit cases. In addition, solutions are investigated numerically for the case of self-interacting BEC beyond the TF limit. We have also analyzed the temporal evolution of density perturbation of BEC DM using derived solutions. Here, we reviewed elaborately and confirmed the results of previous works (notably Refs. [66, 82]), where the evolutionary nature of density contrast is studied in terms of the scale factor. Finally, we conclude that an enhanced comprehension of the numerical attributes linked with BEC parameters could significantly contribute to achieving precise cosmological inferences within the context of the BEC model. Such a progression might also furnish an eloquent approach for empirically scrutinizing the theoretical conjecture of the BEC model, along with exploring the potential presence of condensate DM on a cosmological magnitude.

Acknowledgements One of the authors (SM) is thankful to Govt. of West Bengal, India, for granting the non-NET Ph.D. Swami Vivekananda Merit-cum-Means (SVMCM) Scholarship (up to 16.08.2023). SM also acknowledges Govt. of West Bengal, India, for granting the State-Funded Junior Research Fellowship (JRF) at present.

Data availability statement No new data were created or analyzed in this study.

Declarations

Conflict of interest The authors declare that they have no conflicts of interest.

Open Access This article is licensed under a Creative Commons Attribution 4.0 International License, which permits use, sharing, adaptation, distribution and reproduction in any medium or format, as long as you give appropriate credit to the original author(s) and the source, provide a link to the Creative Commons licence, and indicate if changes were made. The images or other third party material in this article

are included in the article's Creative Commons licence, unless indicated otherwise in a credit line to the material. If material is not included in the article's Creative Commons licence and your intended use is not permitted by statutory regulation or exceeds the permitted use, you will need to obtain permission directly from the copyright holder. To view a copy of this licence, visit <http://creativecommons.org/licenses/by/4.0/>.

Funded by SCOAP³.

References

1. D. Tong, Cambridge University (2019). <http://www.damtp.cam.ac.uk/user/tong/cosmo.html>
2. E.W. Kolb, M.S. Turner, *The Early Universe* (CRC Press, 2018). <https://doi.org/10.1201/9780429492860>
3. J.H. Jeans, Philos. Trans. R. Soc. A **199**, 1 (1902). <https://doi.org/10.1098/rsta.1902.0012>
4. J. Jeans, *Astronomy and Cosmogony* (CUP Archive, 1929). <https://doi.org/10.1017/CBO9780511694363>
5. G.F. Ellis, Gen. Relativ. Gravit. **49**, 1 (2017). <https://doi.org/10.1007/s10714-016-2164-9>
6. W.B. Bonnor, Zeitschrift für Astrophysik **39**, 143 (1956). <https://articles.adsabs.harvard.edu/pdf/1956ZA.....39..143B>
7. S. Perlmutter, G. Aldering, G. Goldhaber, R. Knop, P. Nugent, P.G. Castro, S. Deustua, S. Fabbro, A. Goobar, D.E. Groom et al., Astrophys. J. **517**, 565 (1999). <https://doi.org/10.1086/307221>
8. P. de Bernardis, P.A. Ade, J.J. Bock, J. Bond, J. Borrill, A. Boscaleri, K. Coble, B. Crill, G. De Gasperis, P. Farese et al., Nature **404**, 955 (2000). <https://doi.org/10.1038/35010035>
9. G. Bertone, D. Hooper, J. Silk, Phys. Rep. **405**, 279 (2005). <https://doi.org/10.1016/j.physrep.2004.08.031>
10. B. Sadoulet, Rev. Mod. Phys. **71**, S197 (1999). <https://doi.org/10.1103/RevModPhys.71.S197>
11. G. Jungman, M. Kamionkowski, K. Griest, Phys. Rep. **267**, 195 (1996). [https://doi.org/10.1016/0370-1573\(95\)00058-5](https://doi.org/10.1016/0370-1573(95)00058-5)
12. J. Binney, S. Tremaine, *Galactic Dynamics*, vol. 20 (Princeton University Press, Princeton, 2011)
13. M. Crăciun, T. Harko, Eur. Phys. J. C **80**, 1 (2020). <https://doi.org/10.1140/epjc/s10052-020-8272-4>
14. R. Massey, T. Kitching, J. Richard, Rep. Prog. Phys. **73**, 086901 (2010). <https://doi.org/10.1088/0034-4885/73/8/086901>
15. A.G. Riess, A.V. Filippenko, P. Challis, A. Clocchiatti, A. Diercks, P.M. Garnavich, R.L. Gilliland, C.J. Hogan, S. Jha, R.P. Kirshner et al., Astron. J. **116**, 1009 (1998). <https://doi.org/10.1086/300499>
16. L. Page, M. Nolta, C. Barnes, C. Bennett, M. Halpern, G. Hinshaw, N. Jarosik, A. Kogut, M. Limon, S. Meyer et al., Astrophys. J. Suppl. **148**, 233 (2003). <https://doi.org/10.1086/377224>
17. F. Bernardeau, S. Colombi, E. Gaztanaga, R. Scoccimarro, Phys. Rep. **367**, 1 (2002). [https://doi.org/10.1016/S0370-1573\(02\)00135-7](https://doi.org/10.1016/S0370-1573(02)00135-7)
18. P. Bull et al., Phys. Dark Univ. **12**, 56 (2016). <https://doi.org/10.1016/j.dark.2016.02.001>
19. R.H. Cyburt, B.D. Fields, K.A. Olive, T.-H. Yeh, Rev. Mod. Phys. **88**, 015004 (2016). <https://doi.org/10.1103/RevModPhys.88.015004>
20. G. Steigman, Annu. Rev. Nucl. Part. Sci. **57**, 463 (2007). <https://doi.org/10.1146/annurev.nucl.56.080805.140437>
21. R.H. Cyburt, B.D. Fields, K.A. Olive, T.-H. Yeh, Rev. Mod. Phys. **88**, 015004 (2016). <https://doi.org/10.1103/RevModPhys.88.015004>
22. F. Iocco, G. Mangano, G. Miele, O. Pisanti, P.D. Serpico, Phys. Rep. **472**, 1 (2009). <https://doi.org/10.1016/j.physrep.2009.02.002>
23. M. Abdullah, H. Abele, D. Akimov, G. Angloher, D. Aristizabal-Sierra, C. Augier, A. Balantekin, L. Balogh, P. Barbeau, L. Baudis, et al., (2022). <https://doi.org/10.48550/arXiv.2203.07361>
24. L.A. Anchordoqui, E. Di Valentino, S. Pan, W. Yang, J. High Energy Astrophys. **32**, 28 (2021). <https://doi.org/10.1016/j.jheap.2021.08.001>
25. T. Buchert, A.A. Coley, H. Kleinert, B.F. Roukema, D.L. Wiltshire, Int. J. Mod. Phys. D **25**, 1630007 (2016). <https://doi.org/10.1142/S021827181630007X>
26. K. Schmitz, *Modern Cosmology, An Amuse-Gueule* (Springer, 2022), pp. 37–70. https://doi.org/10.1007/978-3-031-05625-3_3
27. E. Di Valentino, O. Mena, S. Pan, L. Visinelli, W. Yang, A. Melchiorri, D.F. Mota, A.G. Riess, J. Silk, Class. Quantum Gravity **38**, 153001 (2021). <https://doi.org/10.1088/1361-6382/ac086d>
28. S. Weinberg, Rev. Mod. Phys. **61**, 1 (1989). <https://doi.org/10.1103/RevModPhys.61.1>
29. J. Martin, C. R. Phys. **13**, 566 (2012). <https://doi.org/10.1016/j.crhy.2012.04.008>
30. C. Burgess, Post-Planck Cosmol. **100**, 148 (2015). <https://doi.org/10.1093/acprof:oso/9780198728856.003.0004>
31. V.L. Fitch, D.R. Marlow, M.A. Dementi, *Critical Problems in Physics*, vol. 34 (Princeton University Press, Princeton, 2021). <https://doi.org/10.1515/9780691227498>
32. H.E. Velten, R. Vom Martens, W. Zimdahl, Eur. Phys. J. C **74**, 1 (2014). <https://doi.org/10.1140/epjc/s10052-014-3160-4>
33. A.G. Riess, Nat. Rev. Phys. **2**, 10 (2020). <https://doi.org/10.1038/s42254-019-0137-0>
34. K.C. Wong, S.H. Suyu, G.C. Chen, C.E. Rusu, M. Millon, D. Sluse, V. Bonvin, C.D. Fassnacht, S. Taubenberger, M.W. Auger et al., Mon. Not. R. Astron. **498**, 1420 (2020). <https://doi.org/10.1093/mnras/stz3094>
35. D.J. Schwarz, C.J. Copi, D. Huterer, G.D. Starkman, Class. Quantum Gravity **33**, 184001 (2016). <https://doi.org/10.1088/0264-9381/33/18/184001>
36. Y. Akrami, M. Ashdown, J. Aumont, C. Baccigalupi, M. Ballardini, A.J. Banday, R. Barreiro, N. Bartolo, S. Basak, K. Benabed et al., Astron. Astrophys. **641**, A7 (2020). <https://doi.org/10.1051/0004-6361/201935201>
37. J. Evslin, J. Cosmol. Astropart. Phys. **2017**, 024 (2017). <https://doi.org/10.1088/1475-7516/2017/04/024>
38. G. Addison, D. Watts, C. Bennett, M. Halpern, G. Hinshaw, J. Weiland, Astrophys. J. **853**, 119 (2018). <https://doi.org/10.3847/1538-4357/aaa1ed>
39. A. Cuceu, J. Farr, P. Lemos, A. Font-Ribera, J. Cosmol. Astropart. Phys. **2019**, 044 (2019). <https://doi.org/10.1088/1475-7516/2019/10/044>
40. L. Perivolaropoulos, F. Skara, New Astron. Rev. **95**, 101659 (2022). <https://doi.org/10.1016/j.newar.2022.101659>
41. P. Kroupa, B. Famaey, K.S. de Boer, J. Dabringhausen, M. Pawłowski, C.M. Boily, H. Jerjen, D. Forbes, G. Hensler, M. Metz, Astron. Astrophys. **523**, A32 (2010). <https://doi.org/10.1051/0004-6361/201014892>
42. D.H. Weinberg, J.S. Bullock, F. Governato, R. Kuzio de Naray, A.H. Peter, PNAS **112**, 12249 (2015). <https://doi.org/10.1073/pnas.1308716112>
43. T. Nakama, J. Chluba, M. Kamionkowski, Phys. Rev. D **95**, 121302 (2017). <https://doi.org/10.1103/PhysRevD.95.121302>
44. J.S. Bullock, M. Boylan-Kolchin, Annu. Rev. Astron. Astrophys. **55**, 343 (2017). <https://doi.org/10.1146/annurev-astro-091916-055313>
45. A. Del Popolo, M. Le Delliou, Galaxies **5**, 17 (2017). <https://doi.org/10.3390/galaxies5010017>
46. P. Salucci, Astron. Astrophys. Rev. **27**, 1 (2019). <https://doi.org/10.1007/s00159-018-0113-1>
47. W. De Blok, Adv. Astron. **2010**, 789293 (2010). <https://doi.org/10.1155/2010/789293>

48. R.A. Flores, J.R. Primack, *Astrophys. J.* **427**, L1 (1994). <https://doi.org/10.1086/187350>
49. B. Moore, *Nature* **370**, 629 (1994). <https://doi.org/10.1038/370629a0>
50. F. Lelli, *Nat. Astron.* **6**, 35 (2022). <https://doi.org/10.1038/s41550-021-01562-2>
51. I. Ferrero, M.G. Abadi, J.F. Navarro, L.V. Sales, S. Gurovich, *Mon. Not. R. Astron. Soc.* **425**, 2817 (2012). <https://doi.org/10.1111/j.1365-2966.2012.21623.x>
52. B. Moore, T. Quinn, F. Governato, J. Stadel, G. Lake, *Mon. Not. R. Astron. Soc.* **310**, 1147 (1999). <https://doi.org/10.1046/j.1365-8711.1999.03039.x>
53. J.F. Navarro, V.R. Eke, C.S. Frenk, *Mon. Not. R. Astron. Soc.* **283**, L72 (1996). <https://doi.org/10.1093/mnras/283.3.L72>
54. J.F. Navarro, C.S. Frenk, S.D. White, *Astrophys. J.* **490**, 493 (1997). <https://doi.org/10.1086/304888>
55. N. Amorisco, N. Evans, *Mon. Not. R. Astron. Soc.* **419**, 184 (2012). <https://doi.org/10.1111/j.1365-2966.2011.19684.x>
56. G. Battaglia, A. Helmi, E. Tolstoy, M. Irwin, V. Hill, P. Jablonka, *Astrophys. J.* **681**, L13 (2008). <https://doi.org/10.1086/590179>
57. M. Davis, G. Efstathiou, C.S. Frenk, S.D. White, *Astrophys. J.* **292**, 371 (1985). <https://doi.org/10.1086/163168>
58. M.G. Walker, J. Penarrubia, *Astrophys. J.* **742**, 20 (2011). <https://doi.org/10.1088/0004-637X/742/1/20>
59. G. Kauffmann, S.D. White, B. Guiderdoni, *Mon. Not. R. Astron. Soc.* **264**, 201 (1993). <https://doi.org/10.1093/mnras/264.1.201>
60. A. Klypin, A.V. Kravtsov, O. Valenzuela, F. Prada, *Astrophys. J.* **522**, 82 (1999). <https://doi.org/10.1086/307643>
61. B. Moore, S. Ghigna, F. Governato, G. Lake, T. Quinn, J. Stadel, P. Tozzi, *Astrophys. J.* **524**, L19 (1999). <https://doi.org/10.1086/312287>
62. J. Bullock, *Local Group Cosmol.* **20**, 95 (2013). <https://doi.org/10.1017/CBO9781139152303.004>
63. M. Mateo, *Annu. Rev. Astron. Astrophys.* **36**, 435 (1998). <https://doi.org/10.1146/annurev.astro.36.1.435>
64. D.N. Spergel, P.J. Steinhardt, *Phys. Rev. Lett.* **84**, 3760 (2000). <https://doi.org/10.1103/PhysRevLett.84.3760>
65. W. Hu, R. Barkana, A. Gruzinov, *Phys. Rev. Lett.* **85**, 1158 (2000). <https://doi.org/10.1103/PhysRevLett.85.1158>
66. A. Suárez, P.-H. Chavanis, *Phys. Rev. D* **92**, 023510 (2015). <https://doi.org/10.1103/PhysRevD.92.023510>
67. W.H. Press, B.S. Ryden, D.N. Spergel, *Phys. Rev. Lett.* **64**, 1084 (1990). <https://doi.org/10.1103/PhysRevLett.64.1084>
68. J.A. Frieman, C.T. Hill, R. Watkins, *Phys. Rev. D* **46**, 1226 (1992). <https://doi.org/10.1103/PhysRevD.46.1226>
69. S.-J. Sin, *Phys. Rev. D* **50**, 3650 (1994). <https://doi.org/10.1103/PhysRevD.50.3650>
70. S.U. Ji, S.J. Sin, *Phys. Rev. D* **50**, 3655 (1994). <https://doi.org/10.1103/PhysRevD.50.3655>
71. A. Einstein, *Sitzungsber. Kgl. Preuss. Akad. Wiss* **3**, 245 (1925). <https://doi.org/10.1002/3527608958.ch28>
72. S.N. Bose, *Z. Physik* **26**, 178 (1924). <https://doi.org/10.1007/BF01327326>
73. C.C. Bradley, C.A. Sackett, J.J. Tollett, R.G. Hulet, *Phys. Rev. Lett.* **79**, 1170 (1997). <https://doi.org/10.1103/PhysRevLett.79.1170>
74. M.H. Anderson, J.R. Ensher, M.R. Matthews, C.E. Wieman, E.A. Cornell, *Science* **269**, 198 (1995). <https://doi.org/10.1126/science.269.5221.198>
75. C.C. Bradley, C.A. Sackett, R.G. Hulet, *Phys. Rev. Lett.* **78**, 985 (1997). <https://doi.org/10.1103/PhysRevLett.78.985>
76. M. Membrado, A. Pacheco, J. Sañudo, *Astron. Astrophys.* **217**, 92 (1989). <https://ui.adsabs.harvard.edu/abs/1989A&A...217...92M>
77. A. Arbey, J. Lesgourgues, P. Salati, *Phys. Rev. D* **68**, 023511 (2003). <https://doi.org/10.1103/PhysRevD.68.023511>
78. K.R. Jones, D. Bernstein, *Class. Quantum Gravity* **18**, 1513 (2001). <https://doi.org/10.1088/0264-9381/18/8/308>
79. P. Peebles, *Astrophys. J.* **534**, L127 (2000). <https://doi.org/10.1086/312677>
80. M. Silverman, R.L. Mallett, *Gen. Relativ. Gravit.* **34**, 633 (2002). <https://doi.org/10.1023/A:1015934027224>
81. C. Boehmer, T. Harko, *J. Cosmol. Astropart. Phys.* **2007**, 025 (2007). <https://doi.org/10.1088/1475-7516/2007/06/025>
82. P.-H. Chavanis, *Astron. Astrophys.* **537**, A127 (2012). <https://doi.org/10.1051/0004-6361/201116905>
83. T. Harko, *J. Cosmol. Astropart. Phys.* **2011**, 022 (2011). <https://doi.org/10.1088/1475-7516/2011/05/022>
84. T. Harko, *Phys. Rev. D* **83**, 123515 (2011). <https://doi.org/10.1103/PhysRevD.83.123515>
85. S. Das, R.K. Bhaduri, *Class. Quantum Gravity* **32**, 105003 (2015). <https://doi.org/10.1088/0264-9381/32/10/105003>
86. S. Das, R.K. Bhaduri, (2018). <https://doi.org/10.48550/arXiv.1808.10505>
87. M. Morikawa, in *22nd Texas Symposium on Relativistic Astrophysics, Stanford* (2004), pp. 13–17. <https://www.slac.stanford.edu/econf/C041213/papers/1122.PDF>
88. K. Atazadeh, F. Darabi, M. Mousavi, *Eur. Phys. J. C* **76**, 1 (2016). <https://doi.org/10.1140/epjc/s10052-016-4182-x>
89. R. Freitas, S. Gonçalves, *J. Cosmol. Astropart. Phys.* **2013**, 049 (2013). <https://doi.org/10.1088/1475-7516/2013/04/049>
90. T. Fukuyama, M. Morikawa, T. Tatekawa, *J. Cosmol. Astropart. Phys.* **2008**, 033 (2008). <https://doi.org/10.1088/1475-7516/2008/06/033>
91. T. Harko, *Mon. Not. R. Astron. Soc.* **413**, 3095 (2011). <https://doi.org/10.1111/j.1365-2966.2011.18386.x>
92. P. Sikivie, Q. Yang, *Phys. Rev. Lett.* **103**, 111301 (2009). <https://doi.org/10.1103/PhysRevLett.103.111301>
93. B. Kain, H.Y. Ling, *Phys. Rev. D* **85**, 023527 (2012). <https://doi.org/10.1103/PhysRevD.85.023527>
94. P.-H. Chavanis, *Phys. Rev. D* **84**, 043531 (2011). <https://doi.org/10.1103/PhysRevD.84.043531>
95. P.-H. Chavanis, L. Delfini, *Phys. Rev. D* **84**, 043532 (2011). <https://doi.org/10.1103/PhysRevD.84.043532>
96. C.J. Pethick, H. Smith, *Bose-Einstein condensation in dilute gases* (Cambridge University Press, Cambridge, 2008). <https://doi.org/10.1017/CBO9780511802850>
97. H. Velten, E. Wamba, *Phys. Lett. B* **709**, 1 (2012). <https://doi.org/10.1016/j.physletb.2012.01.071>
98. F. Dalfovo, S. Giorgini, L.P. Pitaevskii, S. Stringari, *Rev. Mod. Phys.* **71**, 463 (1999). <https://doi.org/10.1103/RevModPhys.71.463>
99. A. Mohamadou, E. Wamba, S.Y. Doka, T.B. Ekogo, T.C. Kofane, *Phys. Rev. A* **84**, 023602 (2011). <https://doi.org/10.1103/PhysRevA.84.023602>
100. E. Wamba, A. Mohamadou, T.C. Kofane, *Phys. Rev. E* **77**, 046216 (2008). <https://doi.org/10.1103/PhysRevE.77.046216>
101. E. Madelung, *Z. Physik* **40**, 322 (1927). <https://doi.org/10.1007/BF01400372>
102. A.H. Guth, *Phys. Rev. D* **23**, 347 (1981). <https://doi.org/10.1103/PhysRevD.23.347>
103. G. Efstathiou, S. Gratton, *Mon. Not. R. Astron. Soc. Lett.* **496**, L91 (2020). <https://doi.org/10.1093/mnrasl/slaa093>
104. H. Mo, F. Van den Bosch, S. White, *Galaxy Formation and Evolution* (Cambridge University Press, Cambridge, 2010). <https://doi.org/10.1017/CBO9780511807244>
105. J.A. Peacock, *Cosmological Physics* (Cambridge University Press, Cambridge, 1999). <https://doi.org/10.1017/CBO9780511804533>
106. V.F. Mukhanov, V. Mukhanov, M. Viatcheslav, *Physical Foundations of Cosmology* (Cambridge University Press,

- Cambridge, 2005). https://sites.astro.caltech.edu/~george/ay21/readings/Mukhanov_PhysFoundCosm.pdf
107. S. Cotsakis, E. Papantonopoulos, *Cosmological Crossroads: An Advanced Course in Mathematical, Physical and String Cosmology*, vol. 592 (Springer Science & Business Media, 2002). <https://doi.org/10.1007/3-540-48025-0>
 108. W. Bonnor, Mon. Not. R. Astron. Soc. **117**, 104 (1957). <https://doi.org/10.1093/mnras/117.1.104>
 109. S. Weinberg, *Gravitation and Cosmology: Principles and Applications of the General Theory of Relativity* (Wiley, 1972). https://cdn.preterhuman.net/texts/science_and_technology/physics/General_Relativity_Theory/Gravitation
 110. C.J. Hogan, J.J. Dalcanton, Phys. Rev. D **62**, 063511 (2000). <https://doi.org/10.1103/PhysRevD.62.063511>
 111. J. Madsen, Phys. Rev. D **64**, 027301 (2001). <https://doi.org/10.1103/PhysRevD.64.027301>
 112. J.O. Andersen, Rev. Mod. Phys. **76**, 599 (2004). <https://doi.org/10.1103/RevModPhys.76.599>
 113. E.H. Lieb, R. Seiringer, J. Yngvason, Phys. Rev. Lett. **94**, 080401 (2005). <https://doi.org/10.1103/PhysRevLett.94.080401>
 114. L. Olivares-Quiroz, V. Romero-Rochin, J. Phys. B At. Mol. Opt. Phys. **43**, 205302 (2010). <https://doi.org/10.1088/0953-4075/43/20/205302>
 115. J.-H. Park, S.-W. Kim, Phys. Rev. A **81**, 063636 (2010). <https://doi.org/10.1103/PhysRevA.81.063636>
 116. G. Hinshaw, J. Weiland, R. Hill, N. Odegard, D. Larson, C. Bennett, J. Dunkley, B. Gold, M. Greason, N. Jarosik et al., Astrophys. J. Suppl. Ser. **180**, 225 (2009). <https://doi.org/10.1088/0067-0049/180/2/225>
 117. M. Carmeli, J.G. Hartnett, F.J. Oliveira, Found. Phys. Lett. **19**, 277 (2006). <https://doi.org/10.1007/s10702-006-0518-3>
 118. T. Padmanabhan, *Structure Formation in the Universe* (Cambridge University Press, Cambridge, 1993). <https://www.cambridge.org/us/universitypress/subjects/physics/particle-physics-and-nuclear-physics/structure-formation-universe?format=PB&isbn=9780521424868>
 119. M. Abramowitz, *Handbook Of Mathematical Functions With Formulas, Graphs, And Mathematical Tables* (Dover Publications Inc., 1974). <https://doi.org/10.1119/1.15378>
 120. J.D. Jackson, *Classical Electrodynamics* (Wiley, 2021)
 121. J.R. Primack, New J. Phys. **11**, 105029 (2009). <https://doi.org/10.1088/1367-2630/11/10/105029>
 122. A. Burkert, Astrophys. J. **447**, L25 (1995). <https://doi.org/10.1086/309560>
 123. J.F. Navarro, C.S. Frenk, S.D. White, Astrophys. J. **462**, 563 (1996). <https://doi.org/10.1086/177173>
 124. P.J.E. Peebles, B. Ratra, Rev. Mod. Phys. **75**, 559 (2003). <https://doi.org/10.1103/RevModPhys.75.559>
 125. F.E. Schunck, E.W. Mielke, Class. Quantum Gravity **20**, R301 (2003). <https://doi.org/10.1088/0264-9381/20/20/201>
 126. E.W. Mielke, F.E. Schunck, Nucl. Phys. B **564**, 185 (2000). <https://doi.org/10.1016/S0550-3213>